

# The Probability Distribution of Sea Surface Wind Speeds. Part I: Theory and SeaWinds Observations

ADAM HUGH MONAHAN

*School of Earth and Ocean Sciences, University of Victoria, Victoria, British Columbia, and Earth System Evolution Program, Canadian Institute for Advanced Research, Toronto, Ontario, Canada*

(Manuscript received 2 December 2004, in final form 25 May 2005)

## ABSTRACT

The probability distribution of sea surface wind speeds,  $w$ , is considered. Daily SeaWinds scatterometer observations are used for the characterization of the moments of sea surface winds on a global scale. These observations confirm the results of earlier studies, which found that the two-parameter Weibull distribution provides a good (but not perfect) approximation to the probability density function of  $w$ . In particular, the observed and Weibull probability distributions share the feature that the skewness of  $w$  is a concave upward function of the ratio of the mean of  $w$  to its standard deviation. The skewness of  $w$  is positive where the ratio is relatively small (such as over the extratropical Northern Hemisphere), the skewness is close to zero where the ratio is intermediate (such as the Southern Ocean), and the skewness is negative where the ratio is relatively large (such as the equatorward flank of the subtropical highs). An analytic expression for the probability density function of  $w$ , derived from a simple stochastic model of the atmospheric boundary layer, is shown to be in good qualitative agreement with the observed relationships between the moments of  $w$ . Empirical expressions for the probability distribution of  $w$  in terms of the mean and standard deviation of the vector wind are derived using Gram–Charlier expansions of the joint distribution of the sea surface wind vector components. The significance of these distributions for improvements to calculations of averaged air–sea fluxes in diagnostic and modeling studies is discussed.

## 1. Introduction

Models of the probability distribution of sea surface wind speeds play a central role in a number of problems in meteorology, oceanography, and climate; these include wind power meteorology (Petersen et al. 1998a,b), remote sensing of sea surface winds (e.g., Wentz et al. 1984; Meissner et al. 2001), and estimates of air–sea exchanges of heat, momentum, moisture, and gases (e.g., Wright and Thompson 1983; Thompson et al. 1983; Isemer and Hasse 1991; Wanninkhof 1992; Wanninkhof and McGillis 1999; Taylor 2000; Wanninkhof et al. 2002). In particular, turbulent air–sea fluxes depend on eddy-averaged quantities such as the friction or piston velocities, which for many applications are parameterized in terms of the sea surface wind speed. These bulk parameterizations of air–sea fluxes

are typically nonlinear in the sea surface wind speed, so the space or time average flux is not generally equal to the flux that would be diagnosed from the averaged wind. In fact, the average flux will generally depend on higher-order moments of the sea surface wind speed, such as the standard deviation and skewness. From both diagnostic and modeling perspectives, there is a need for parameterizations of the probability distribution of sea surface wind speeds.

A number of empirical studies have demonstrated that surface wind speed distributions over both land and sea can be well represented by the two-parameter Weibull distribution (Hennessey 1977; Justus et al. 1978; Conradsen et al. 1984; Isemer and Hasse 1991; Deaves and Lines 1997; Pang et al. 2001), although it has been noted that the fit is not exact (e.g., Stewart and Essenswanger 1978; Takle and Brown 1978; Tuller and Brett 1984; Erickson and Taylor 1989; Bauer 1996). Most previous efforts to characterize wind speed probability distributions in both coastal (e.g., Dixon and Swift 1984; Tuller and Brett 1984; Pryor and Barthelmie 2002) and open-ocean (e.g., Pavia and O'Brien 1986;

---

*Corresponding author address:* Dr. Adam Hugh Monahan, School of Earth and Ocean Sciences, University of Victoria, P.O. Box 3055 STN CSC, Victoria, BC V8P 5C2, Canada.  
E-mail: monahana@uvic.ca

Isemer and Hasse 1991) locations have relied on data from in situ observations and have thus been constrained by limited sampling in both space and time. In particular, the study of seasonal and latitudinal variation of Weibull parameters by Pavia and O'Brien (1986) used ship-based wind speed observations from a single year (1983), with very poor spatial resolution over the tropical and Southern Hemisphere oceans. In contrast, the study of Isemer and Hasse (1991) used over 30 years' worth of ship-based wind speed estimates obtained from visual inspection of the sea state, but this analysis was limited to the North Atlantic.

A new era in the study of sea surface wind speeds began with the advent of satellite anemometry, using both active and passive remote sensing devices (e.g., Atlas et al. 1996; Bentamy et al. 1999; Kelly 2004). Satellite-borne instruments have provided global observations of sea surface winds with unprecedentedly high resolution in space and time, allowing statistically significant characterization of the probability density functions (PDFs) of surface wind speeds in previously poorly sampled oceanic regions. In general, remotely sensed sea surface wind speeds agree reasonably well with in situ observations and surface analysis fields, although some biases (dependent on region and wind speed) are found (e.g., Bentamy et al. 1999; Ebuchi 1999; Meissner et al. 2001; Ebuchi et al. 2002; Bourassa et al. 2003; Curry et al. 2004; Yuan 2004; Chelton and Freilich 2005), some of which are associated with strong sea surface currents (e.g., Kelly et al. 2001, 2005; Chelton et al. 2004). In Bauer (1996), the PDFs of remotely sensed winds for November 1992 were considered, but the short duration of the observations necessitated a coarse spatial resolution of three zonal bins corresponding to the Tropics and to the Northern and Southern Hemisphere extratropics.

The first part of the present study characterizes the spatial structure of both the moments and the best-fit Weibull parameters of 10-m sea surface wind speeds using 6 yr of level 3.0 gridded observations from the SeaWinds scatterometer on the National Aeronautics and Space Administration (NASA) Quick Scatterometer (QuikSCAT) satellite (Jet Propulsion Laboratory 2001). The high temporal and spatial resolution (approximately daily and  $1/4^\circ \times 1/4^\circ$ , respectively) of the dataset, along with its relatively long duration, allows a global characterization of the annual PDFs of sea surface wind speeds. The objective of this part of the present study is not to critique or ground-truth the SeaWinds observations of sea surface winds; such analyses appear in other studies (e.g., Ebuchi et al. 2002; Bourassa et al. 2003; Chelton and Freilich 2005) in which it is demonstrated that SeaWinds observations

of sea surface winds generally agree favorably with in situ buoy and ship observations. Rather, these observations are considered in this study as a source of state-of-the-art data for the characterization of sea surface wind PDFs. Furthermore, we will investigate the extent to which the SeaWinds data are accurately represented by the Weibull distribution. It will be demonstrated that while the data are approximately Weibull, there are systematic deviations from Weibull behavior that cannot be accounted for by sampling variability. A comparison of the PDFs obtained in this study with those derived from other sea surface wind datasets, along with an analysis of the seasonal evolution of the wind speed PDFs, is presented in a companion paper (Monahan 2006, hereafter Part II).

As other authors have noted (e.g., Kestens and Teugels 2002), a limitation of most previous studies of the PDF of sea surface wind speeds is that they have been primarily empirical and have not provided a theoretical explanation of the observed wind speed probability distribution. Several studies (e.g., Tuller and Brett 1984; Wentz et al. 1984; Meissner et al. 2001; Cakmur et al. 2004, hereafter CMT) have noted that a Rayleigh distribution (a special case of the Weibull distribution) arises for the wind speed if the vector wind components are assumed to be individually Gaussian with zero mean and independent, isotropic fluctuations. Under these assumptions, the joint PDF of the zonal and meridional wind components, respectively denoted as  $U$  and  $V$ , is

$$p(U, V) = \frac{1}{2\pi\sigma^2} \exp\left(-\frac{U^2 + V^2}{2\sigma^2}\right), \quad (1)$$

where  $\sigma$  is the standard deviation of both  $U$  and  $V$ . Transforming from the orthogonal coordinates  $U, V$  to the polar coordinates  $w, \phi$  (respectively the wind speed and compass direction),

$$U = w \sin\phi, \quad (2)$$

$$V = w \cos\phi, \quad (3)$$

noting that probability must be conserved under the coordinate transformation:

$$p(U, V) dU dV = p(U, V) w dw d\phi = p(w, \phi) dw d\phi, \quad (4)$$

and integrating over the angle  $\phi$  yields the marginal probability density function for the wind speed alone:

$$p(w) = \int_0^{2\pi} p(w, \phi) d\phi = \frac{w}{\sigma^2} \exp\left(-\frac{w^2}{2\sigma^2}\right). \quad (5)$$

While the assumptions leading to the PDF [Eq. (5)] may be a good approximation globally (although see section 5 below), they certainly are not true in general locally. By the same token, while sea surface wind speeds may be approximately Rayleigh on a global scale (e.g., Meissner et al. 2001; Yuan 2004), this is generally not the case locally or regionally (e.g., Tuller and Brett 1984; Pavia and O'Brien 1986; Bauer 1996; Wanninkhof et al. 2002). A second goal of this study is the development of physical and empirical models of the observed PDF of sea surface wind speed, and the development of analytic expressions for this PDF. In particular, we will demonstrate that the structure of the PDF of  $w$  cannot be accounted for without taking into account the non-Gaussian structure of the vector wind PDF. It was shown in Monahan (2004b) that the zonal and meridional components of the sea surface vector wind are each systematically skewed, such that a component is positively (negatively) skewed when the mean of the component is negative (positive). This spatial anticorrelation of the mean and skewness fields was shown to be a natural consequence of the nonlinear drag law characteristic of the surface boundary layer. We will show that the skewness, as well as the kurtosis, of the surface vector wind components play an important role in determining the PDF of sea surface wind speeds.

The sea surface wind dataset used in this study is described in detail in section 2. A review of the properties of the Weibull distribution is presented in section 3, and a discussion of the observed statistics of the sea surface wind speeds is presented in section 4. Section 5 describes an analysis of the accuracy of the characterization of sea surface wind speeds on a global scale by the Rayleigh distribution. A physically based model of the wind speed PDFs is presented in section 6. This theoretical model is shown to capture essential features of the PDF of sea surface wind speeds, but it is not quantitatively accurate. A class of more quantitatively accurate empirical models is described in section 7. A summary and conclusions are given in section 8.

## 2. Data

The sea surface wind dataset considered in this study consists of level 3.0 gridded daily SeaWinds scatterometer 10-m zonal and meridional wind observations from the NASA QuikSCAT satellite (Jet Propulsion Laboratory 2001), available on a  $1/4^\circ \times 1/4^\circ$  grid from

19 July 1999 to the present (15 March 2005 for the present study). These data are available for download from the NASA Jet Propulsion Laboratory (JPL) Distributed Active Archive Center (see <http://podaac.jpl.nasa.gov>). The SeaWinds data have been extensively compared with buoy and ship measurements of surface winds (Ebuchi et al. 2002; Bourassa et al. 2003; Chelton and Freilich 2005); the root-mean-square errors of the remotely sensed wind speed and direction are both found to depend on wind speed, with average values of  $\sim 1 \text{ m s}^{-1}$  and  $\sim 20^\circ$ , respectively. Because raindrops are effective scatterers of microwaves in the wavelength band used by the SeaWinds scatterometer, rainfall can lead to errors in estimates of sea surface winds. The SeaWinds level 3.0 dataset flags those data points that are estimated as likely to have been corrupted by rain (Jet Propulsion Laboratory 2001); these data points have been excluded from the present analysis. No further processing of the data, such as filtering or removing the annual cycle, was carried out on this dataset.

A second dataset used in this study is the number of observations per month and  $1^\circ \times 1^\circ$  grid box of sea surface wind speed in the Comprehensive Ocean–Atmosphere Data Set (COADS). These data are available for download from the International Research Institute for Climate Prediction/Lamont-Doherty Earth Observatory (IRI/LDEO) Climate Data Library (see <http://ingrid.ldeo.columbia.edu>).

## 3. A brief review of the Weibull distribution

We begin with a brief review of the properties of the Weibull distribution; a more complete discussion is presented in Johnson et al. (1994). A random variable  $x$  characterized by a two-parameter Weibull distribution has the PDF

$$p(x) = \frac{b}{a} \left(\frac{x}{a}\right)^{b-1} \exp\left[-\left(\frac{x}{a}\right)^b\right]. \quad (6)$$

The parameters  $a$  and  $b$  denote, respectively, the scale and shape parameters of the distribution. Averages of powers of  $x$  are given simply by

$$\text{mean}(x^k) = a^k \Gamma\left(1 + \frac{k}{b}\right), \quad (7)$$

where  $\Gamma$  is the gamma function. In particular, the mean, standard deviation, skewness, and kurtosis of  $X$  are given by

$$\text{mean}(x) = a\Gamma\left(1 + \frac{1}{b}\right), \quad (8)$$

$$\text{std}(x) = a\left[\Gamma\left(1 + \frac{2}{b}\right) - \Gamma^2\left(1 + \frac{1}{b}\right)\right]^{1/2}, \quad (9)$$

$$\text{skew}(x) = \frac{\Gamma\left(1 + \frac{3}{b}\right) - 3\Gamma\left(1 + \frac{1}{b}\right)\Gamma\left(1 + \frac{2}{b}\right) + 2\Gamma^3\left(1 + \frac{1}{b}\right)}{\left[\Gamma\left(1 + \frac{2}{b}\right) - \Gamma^2\left(1 + \frac{1}{b}\right)\right]^{3/2}}, \quad \text{and} \quad (10)$$

$$\text{kurt}(x) = \frac{\Gamma\left(1 + \frac{4}{b}\right) - 4\Gamma\left(1 + \frac{3}{b}\right)\Gamma\left(1 + \frac{1}{b}\right) + 6\Gamma\left(1 + \frac{2}{b}\right)\Gamma^2\left(1 + \frac{1}{b}\right) - 3\Gamma^4\left(1 + \frac{1}{b}\right)}{\left[\Gamma\left(1 + \frac{2}{b}\right) - \Gamma^2\left(1 + \frac{1}{b}\right)\right]^2} - 3; \quad (11)$$

where the skewness and kurtosis are, respectively, the normalized third- and fourth-order moments:

$$\text{skew}(x) = \frac{\text{mean}\{[x - \text{mean}(x)]^3\}}{\text{std}^3(x)}, \quad \text{and} \quad (12)$$

$$\text{kurt}(x) = \frac{\text{mean}\{[x - \text{mean}(x)]^4\}}{\text{std}^4(x)} - 3. \quad (13)$$

Skewness is a measure of the asymmetry of a PDF: a positive (negative) skewness of a variable  $x$  indicates that the PDF is characterized by an elongated tail in the direction of positive (negative) fluctuations away from the mean, so the mean of  $x$  is larger (smaller) than the most likely value of  $x$ . A variable  $x$  has positive (negative) kurtosis if its PDF is more sharply peaked (broadly peaked) and has longer (shorter) tails than a Gaussian distribution with the same mean and standard deviation. Both the skewness and kurtosis are zero for a Gaussian distribution.

The dependence of  $\text{mean}(x)$ ,  $\text{std}(x)$ ,  $\text{skew}(x)$ , and  $\text{kurt}(x)$  on the Weibull parameters  $a$  and  $b$  is illustrated in Fig. 1; note in particular that the skewness and kurtosis depend only on the parameter  $b$ . For  $b < 3.6$ , the distribution of  $x$  is positively skewed; for  $b > 3.6$ , the skewness is negative. The kurtosis of  $x$  is close to zero for  $b > 2$  but increases rapidly as  $b$  drops below this value. Note that the Weibull distribution for  $b = 3.6$  is a close approximation to a Gaussian distribution.

It can be shown that

$$\text{mean}(\ln x) = \ln a - \frac{\gamma}{b}, \quad \text{and} \quad (14)$$

$$\text{var}(\ln x) = \frac{\pi^2}{6b^2}, \quad (15)$$

where  $\gamma \approx 0.57721$  is Euler's constant [Conradsen et al. 1984; note the sign error in their Eq. (9)]. Furthermore, Eqs. (8) and (9) can be approximately inverted to yield

$$b \approx \left[\frac{\text{mean}(x)}{\text{std}(x)}\right]^{1.086}, \quad \text{and} \quad (16)$$

$$a = \frac{\text{mean}(x)}{\Gamma(1 + 1/b)} \quad (17)$$

(e.g., Justus et al. 1978).

A number of estimators of Weibull parameters  $a$  and  $b$  exist (Conradsen et al. 1984; Pang et al. 2001); these include

- 1) estimates obtained from Eqs. (14)–(15), using the sample estimates of  $\text{mean}(\ln x)$  and  $\text{std}(\ln x)$ ;
- 2) maximum likelihood estimates (Conradsen et al. 1984), and
- 3) estimates from the approximate Eqs. (16)–(17), using sample estimates of  $\text{mean}(x)$  and  $\text{std}(x)$ .

Monte Carlo experiments using simulated Weibull data (not shown) indicate that each of these estimators is unbiased, although estimator 1 has a relatively large variance. The performances of estimators 2 and 3 are essentially equivalent, so there is no reason in principle to prefer one over the other. Being based on the sample mean and standard deviation, estimator 3 is easiest to compute; this estimator will be used for the remainder of this study.

#### 4. Statistical features of the observed sea surface wind speeds

The mean, standard deviation, skewness, and kurtosis fields of  $w$  estimated from the SeaWinds data are displayed in Fig. 2. Large values of  $\text{mean}(w)$  occur in the westerly belts of the Northern and Southern Hemispheres; secondary maxima in the easterly belt occur on the equatorward flanks of the subtropical highs. Minima of  $\text{mean}(w)$  occur in the equatorial doldrums and subtropical horse latitudes. The standard deviation of  $w$  is largest in the midlatitude extratropics (in the

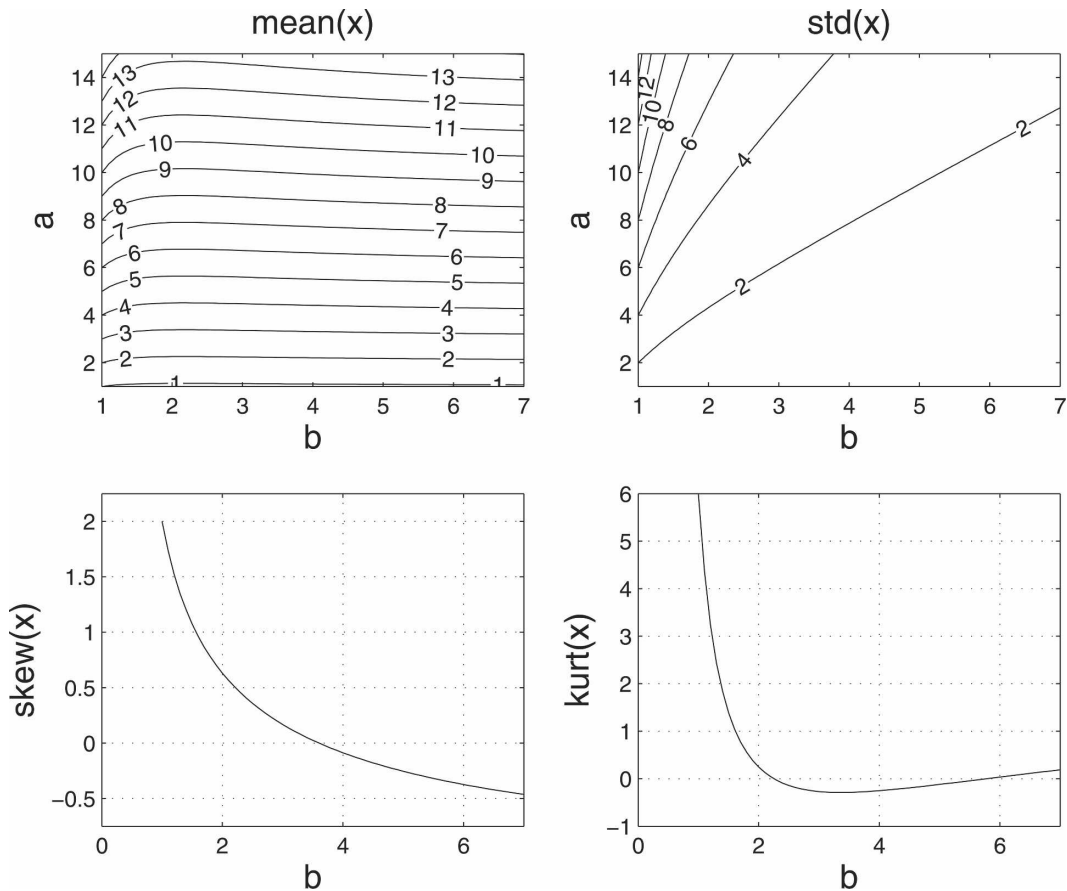


FIG. 1. Dependence of the mean, std dev, skewness, and kurtosis of the Weibull-distributed variable  $x$  on the Weibull parameters  $a$  and  $b$  [Eqs. (8)–(11)].

storm tracks) and generally decreases toward the equator, but with a local maximum along the intertropical convergence zone (ITCZ). In general,  $w$  is positively skewed in the extratropics and negatively skewed in the Tropics, as has been noted by Bauer (1996). Major exceptions to this pattern are the band of positively skewed wind speeds over the tropical Indian Ocean and western Pacific, where mean wind speeds are small, and over the Southern Ocean, where the skewness of  $w$  is generally close to zero. The kurtosis field is much noisier than those of  $\text{mean}(w)$ ,  $\text{std}(w)$ , or  $\text{skew}(w)$ ; this is not surprising, considering the limited duration of the wind speed dataset.

The upper and lower panels in Fig. 3 display, respectively, the Weibull scale and shape parameter fields estimated from the SeaWinds data. The structure of the scale parameter  $a$  field is essentially identical (up to a scaling factor) to that of  $\text{mean}(w)$ , which is to be expected in light of Eq. (8) and Fig. 1. The Weibull shape parameter  $b$  is generally close to 2 throughout the extratropics, rising to between 3 and 4 over the Southern Ocean. Values of  $b$  are generally larger in the Tropics

than in the extratropics, with local extrema (where the value of  $b$  can exceed 5) on the equatorward flanks of the subtropical high pressure cells where the mean winds are strong and the variability is weak [cf. Eq. (16) and Fig. 1]. The association of high values of the Weibull shape parameter with regions of strong and steady winds was noted previously in Pavia and O'Brien (1986, hereafter PO) and Isemer and Hasse (1991).

The distribution of the Weibull  $b$  parameter over the North Atlantic illustrated in Fig. 3 agrees well with the results presented in Isemer and Hasse (1991). Differences between the estimates of the Weibull parameters in this study with those presented in PO are considerably greater. In the northern extratropics, the results of the present study agree reasonably well with those of PO. In the Tropics and Southern Hemisphere extratropics, the differences are considerably larger. Estimates in PO of the shape parameter  $b$  in the Tropics are much smaller than those in the present study; in fact, PO find that  $b$  within a given longitude band is generally a minimum, rather than a maximum, in the Tropics.

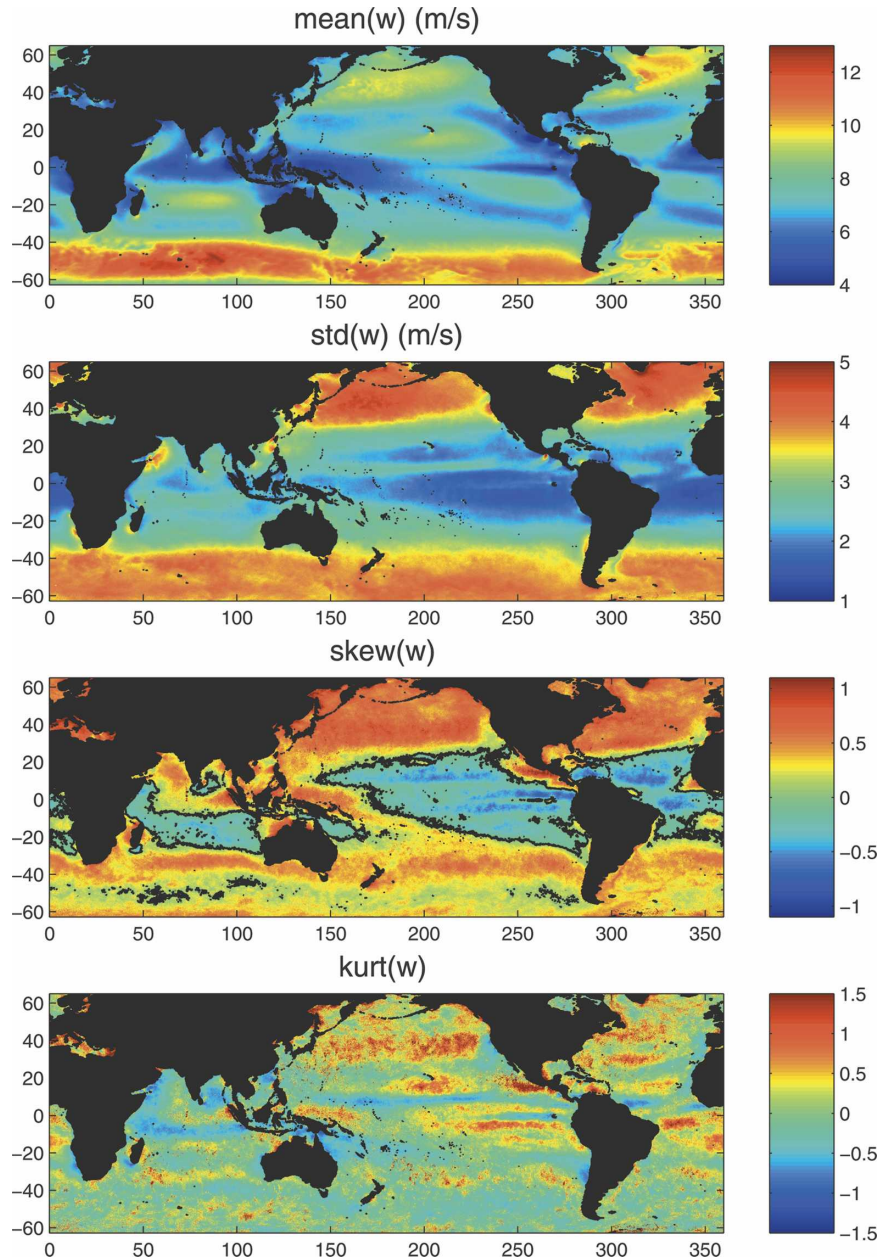


FIG. 2. Mean, std dev, skewness, and kurtosis fields of sea surface wind speed estimated from daily SeaWinds observations. The thick black line in the plot of skew( $w$ ) is the zero contour.

Furthermore, both Weibull  $a$  and  $b$  parameters are generally underestimated over the Southern Ocean in PO as compared to the present study. While the precise dataset used in PO was not available for the present study, the sampling density of their dataset is presumably comparable to that of COADS. The upper panel of Fig. 4 illustrates the number of wind speed observations (per  $1^\circ \times 1^\circ$  grid box) for the year 1983 in the COADS database, on a logarithmic scale; this map resembles a similar map of sampling density presented in

PO. It is evident that while the North Atlantic and subpolar North Pacific Oceans are well sampled, the Tropics (particularly the Pacific) and the Southern Ocean are very poorly sampled. In contrast, the number of observations (per  $1/4^\circ \times 1/4^\circ$  box) is much more uniform in the SeaWinds dataset, as is illustrated in the lower panel of Fig. 4. There are relatively few data in regions of high precipitation where a relatively large number of rain-flagged measurements were rejected [particularly along the ITCZ and South Pacific conver-

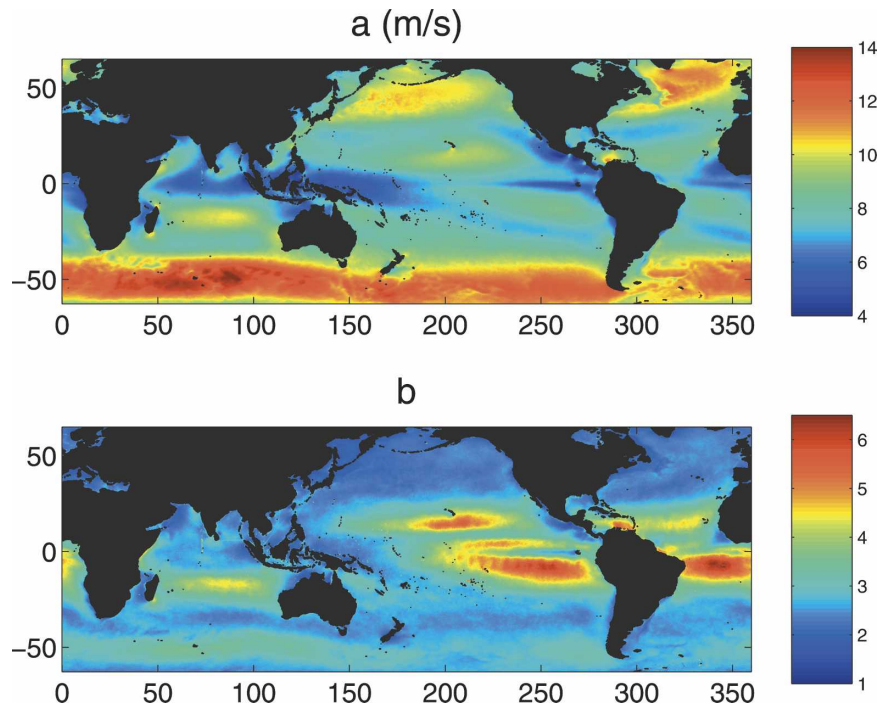


FIG. 3. Same as in Fig. 2, but for Weibull *a* and *b* parameters.

gence zone (SPCZ)], and in meridional bands around 90°E and 90°W resulting from the satellite sampling protocol, but away from the Antarctic ice margin in none of these pixels are there fewer than 1500 obser-

ventions. Throughout the World Ocean, therefore, the present SeaWinds dataset has enough observations to characterize the statistical structure of the sea surface wind speeds (on less than interannual time scales) with

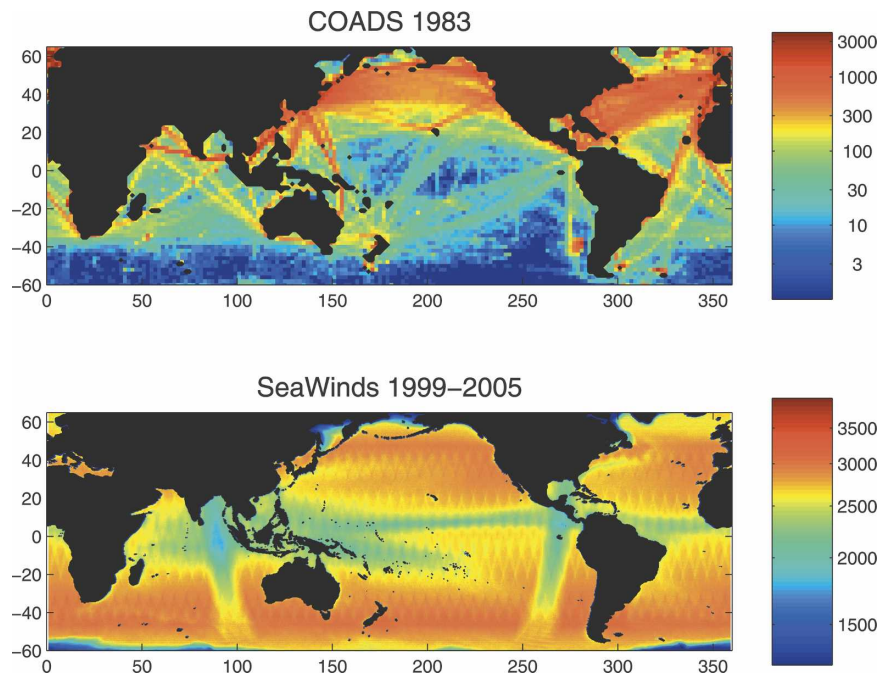


FIG. 4. Number of wind speed observations (top) (per 1° × 1° grid box) in the COADS database for 1983 and (bottom) (per 1/4° × 1/4° grid box) in the SeaWinds database for 1999–2005. Note the logarithmic scales of the two maps.

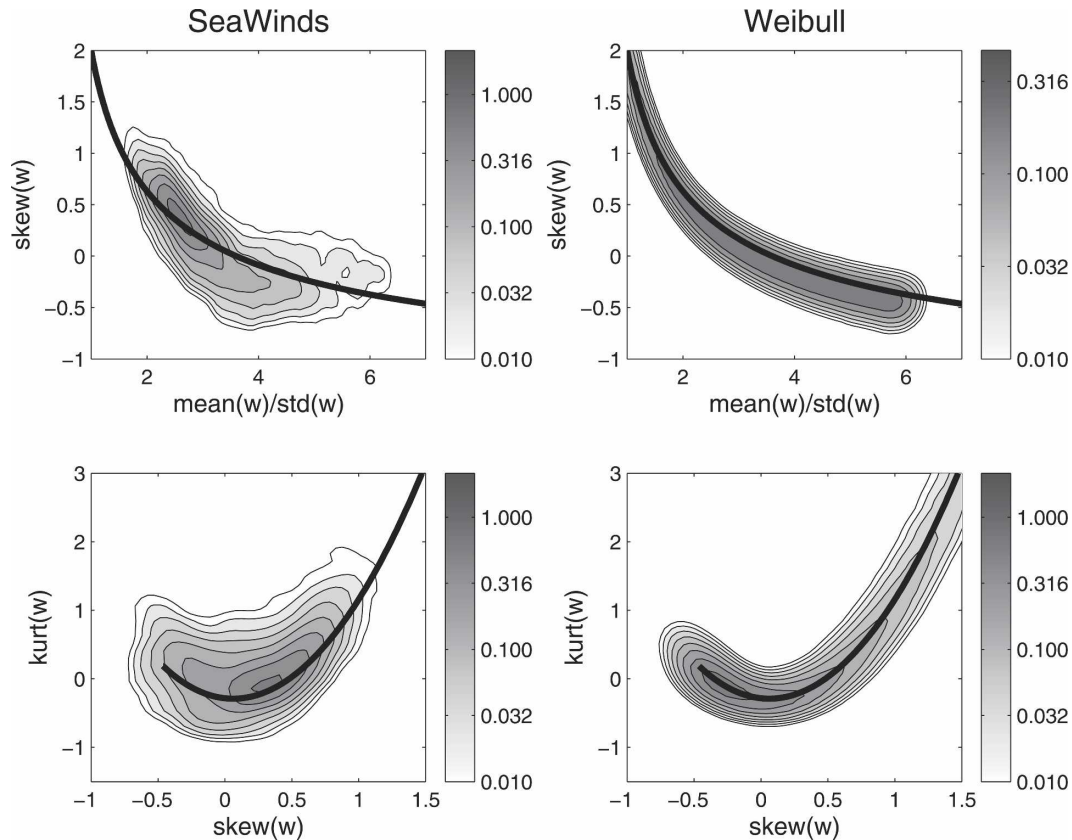


FIG. 5. (top) Kernel density estimates of joint PDFs of  $\text{mean}(w)/\text{std}(w)$  and  $\text{skew}(w)$  for (left) SeaWinds data and (right) synthetic Weibull data. The contour intervals are logarithmically spaced. The thick black line is the theoretical curve for a Weibull variable. (bottom) Same as in top, but for the joint PDF of  $\text{skew}(w)$  and  $\text{kurt}(w)$ .

confidence. In the COADS dataset (which we presume is similar to that used in PO), these regions of high statistical confidence are restricted to the North Atlantic and the subarctic North Pacific. Furthermore, as is clear from Eq. (16) and Fig. 1, small values of  $b$  in the Tropics are inconsistent with the negative skewness of  $w$  in these regions noted in Bauer (1996) and the present study. We conclude that differences between the results of the present study and those of PO arise because of the limited spatial coverage of the dataset used in the earlier study.

The skewness and the shape parameter  $b$  of a Weibull-distributed variable are uniquely related, as is illustrated in Fig. 1. The fact that the map of the shape parameter  $b$  (Fig. 3) reflects the map of the skewness field (Fig. 2) in a manner consistent with this relationship provides evidence that sea surface wind speeds are Weibull to a good approximation; note that only  $\text{mean}(w)$  and  $\text{std}(w)$ , but not  $\text{skew}(w)$ , were used to estimate  $b$ . The relationship between  $\text{skew}(w)$  and the ratio  $\text{mean}(w)/\text{std}(w)$  [which by Eq. (16) is closely related to  $b$ ] is clearly illustrated by the plot of their joint PDF presented in the upper left panel of Fig. 5. The

thick black line represents the theoretical curve for a Weibull variable, Eq. (10). Evidently, in the observations as for a Weibull variable,  $\text{skew}(w)$  is a concave upward function of the ratio  $\text{mean}(w)/\text{std}(w)$ , such that the function is positive for small values of this ratio and negative for large values. Similarly, the relationship between  $\text{skew}(w)$  and  $\text{kurt}(w)$  in the observations is similar to that for a Weibull variable (Fig. 5, lower left panel). From Eqs. (10) and (11) both  $\text{skew}(w)$  and  $\text{kurt}(w)$  for a Weibull variable are determined uniquely by the shape parameter  $b$ , so a plot of  $\text{skew}(w)$  against  $\text{kurt}(w)$  traces out a 1D curve, around which the joint PDF of the observations falls. The agreement between the moment relationships in the SeaWinds data and those for a Weibull variable reinforces the conclusion that these data are Weibull to a good approximation.

Inspection of Fig. 5, however, indicates distinct non-Weibull structure in the PDF of sea surface wind speeds. The upper left panel of Fig. 5 demonstrates that the observed joint PDF of  $\text{mean}(w)/\text{std}(w)$  and  $\text{skew}(w)$  lies above the Weibull curve for low values of the ratio and lies below it for large values. Furthermore, the slope of the relationship between  $\text{skew}(w)$  and the

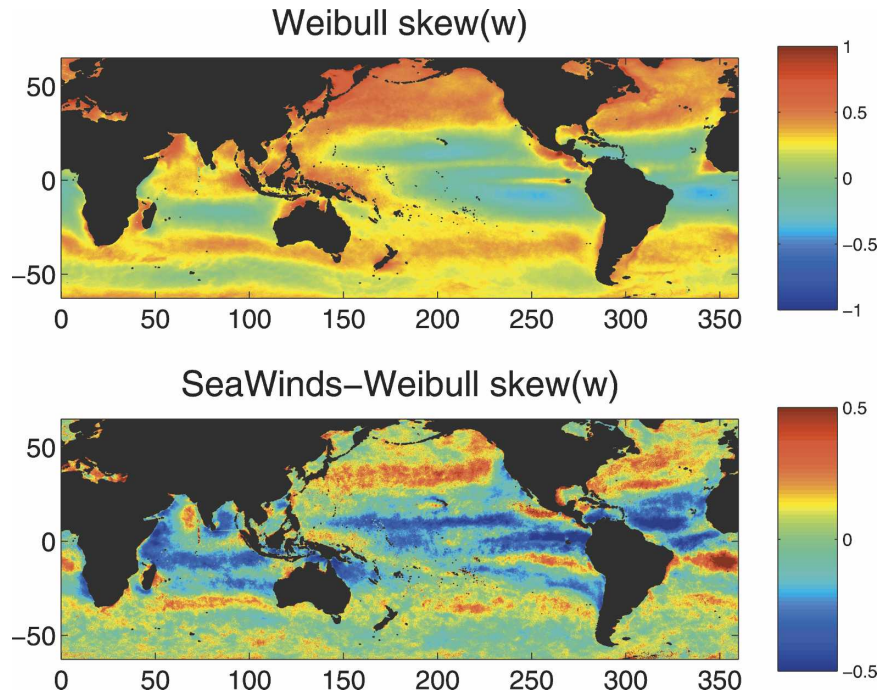


FIG. 6. (top) Map of  $\text{skew}(w)$  for Weibull-distributed variable with  $\text{mean}(w)$  and  $\text{std}(w)$  from SeaWinds observations [cf. Eqs. (10) and (16)]. (bottom) Difference in skewness fields between SeaWinds observations and the equivalent Weibull variable.

ratio  $\text{mean}(w)/\text{std}(w)$  is steeper than the Weibull curve for low values of the ratio and shallower for higher values. A map of the skewness field for the Weibull variable with estimated  $\text{mean}(w)$  and  $\text{std}(w)$  from SeaWinds is presented in the upper panel of Fig. 6. Comparing this field with the SeaWinds  $\text{skew}(w)$  field in Fig. 2, it is clear that the negative skewness in the Tropics is less negative for the Weibull variable than for the SeaWinds data, and that the positive skewness in the NH extratropics is not as positive for the Weibull variable as for the SeaWinds data. These differences are further emphasized in the lower panel of Fig. 6, which displays the difference in skewness fields between the Weibull and SeaWinds variables. The difference field between  $\text{kurt}(w)$  and the Weibull kurtosis field obtained using  $a$  and  $b$  (not shown) is generally positive but is very noisy.

It is of course possible that the wind speeds are Weibull and the apparent non-Weibull structure in the SeaWinds  $\text{skew}(w)$  field arises simply because of sampling variability. To assess the probability of the differences having arisen by chance, a Monte Carlo approach was taken. Values of the Weibull parameters  $a$  and  $b$  were sampled on a regular grid spanning the range of these parameters observed in the SeaWinds data; for each pair, 50 realizations of Weibull time series were randomly generated. Each of these time series con-

sisted of 1000 independent realizations of the random variable; given that at most locations the SeaWinds dataset consists of between 2500 and 3500 daily observations with an autocorrelation  $e$ -folding time of 1–2 days, this number of degrees of freedom is consistent with those of the observations. The right-hand panels of Fig. 5 display estimates of the joint PDFs of  $\text{mean}(w)/\text{std}(w)$  with  $\text{skew}(w)$  (upper panel), and of  $\text{skew}(w)$  with  $\text{kurt}(w)$  (lower panel), as estimated from this synthetic Weibull dataset. When compared to the SeaWinds PDFs, the synthetic Weibull PDFs cluster more tightly and are more symmetrically distributed, around the theoretical Weibull curves. This fact suggests that the deviations from Weibull behavior of the SeaWinds data illustrated in Figs. 5 and 6 are not simply artifacts of sampling variability, but rather reflect actual non-Weibull structure in the SeaWinds characterization of sea surface wind speeds. The possibility remains that the non-Weibull structure is an artifact of the SeaWinds observations. However, the facts that SeaWinds wind observations have been found to be generally in close agreement with buoy and ship observations (e.g., Ebu-chi et al. 2002; Bourassa et al. 2003) and that non-Weibull behavior is evident in other sea surface wind datasets (Part II) suggest that this structure is not spurious. Finally, it is also possible that the wind speeds are Weibull with seasonally varying parameters and that

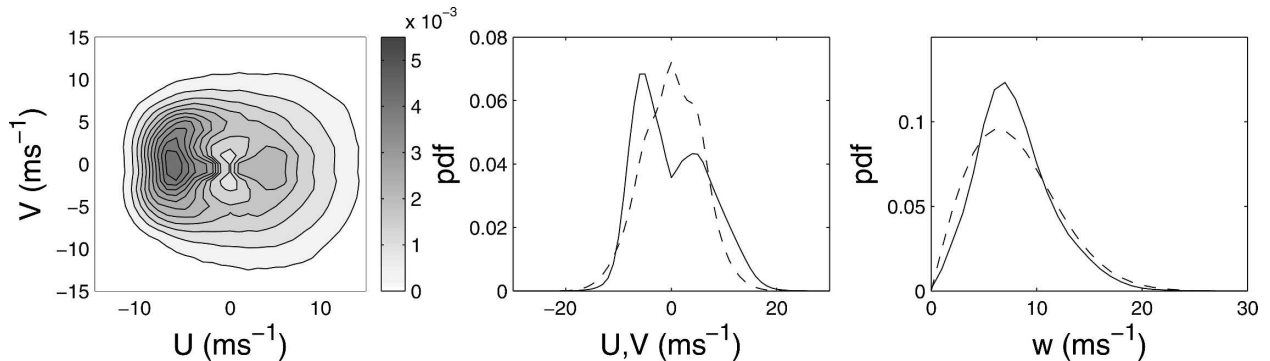


FIG. 7. (left) Joint PDF of observed global zonal and meridional wind components. (middle) Marginal PDFs of observed global zonal (solid line) and meridional (dashed line) wind components. (right) PDF of observed global wind speed (solid line) and best-fit Rayleigh distribution (dashed line).

the apparent non-Weibull structure arises because of this nonstationarity. A seasonally stratified analysis of sea surface wind speeds presented in Part II of this study suggests that the observed non-Weibull structure is not an artifact of nonstationarity.

Erickson and Taylor (1989) used a modified Kolmogorov–Smirnov test to demonstrate statistically significant non-Weibull behavior of surface winds in the coarse resolution National Center for Atmospheric Research (NCAR) Community Climate Model (CCM1). The preceding analysis extends the results of Erickson and Taylor (1989) by considering the structure of observed rather than modeled winds, and by quantifying the differences between the observed wind speed distributions and Weibull distributions, rather than just noting the existence of these differences.

We have thus demonstrated that while the observed sea surface wind speeds deviate systematically from Weibull behavior, the Weibull approximation provides a reasonable first-order characterization of  $\text{mean}(w)$ ,  $\text{std}(w)$ ,  $\text{skew}(w)$ , and  $\text{kurt}(w)$ . This does not guarantee that extreme events are accurately represented by the Weibull distribution; however, averages of polynomial functions of  $w$  are relevant to a broad range of climate and wind power applications (Petersen et al. 1998a,b; Taylor 2000; Jones and Toba 2001; Donelan et al. 2002), for which the correct representation of these moments is adequate. After a brief discussion of the accuracy of the Rayleigh distribution in characterizing global sea surface wind speeds, in section 6 we will proceed to develop a theoretical explanation of the observed relationships between the wind speed field moments.

### 5. How well does the Rayleigh distribution represent global sea surface wind speeds?

The global distribution of sea surface wind speeds is often modeled as a Rayleigh distribution (e.g., Wan-

ninkhof 1992; Wanninkhof and McGillis 1999; Meissner et al. 2001; Yuan 2004), the special case of the Weibull distribution for which  $b = 2$ . As was noted in section 1, this distribution is appropriate if the vector wind components are individually Gaussian with mean zero and independent, isotropic fluctuations. We proceed to investigate the accuracy of the Rayleigh distribution in describing the global distribution of SeaWinds wind speeds and of the validity of the assumptions from which the Rayleigh model rigorously follows.

The joint PDF  $p(U, V)$  of the global zonal and meridional wind components (respectively denoted  $U$  and  $V$ ), obtained from all sea surface grid points, is displayed in the left-hand panel of Fig. 7; note that the structure of  $p(U, V)$  reflects both local and regional variability in the vector wind. Plots of the marginal distributions of  $U$  and  $V$  are given in the center panel of Fig. 7. The marginal distributions of a joint distribution  $p(U, V)$  are the distributions of  $U$  and  $V$  individually, obtained by integrating the joint distribution, respectively, over  $V$  and  $U$ . The anisotropic local minimum in  $p(U, V)$  near  $(U, V) = (0, 0) \text{ m s}^{-1}$  is presumably an artifact of the SeaWinds data; errors in wind direction are known to be greatest at very low wind speeds (e.g., Ebuchi et al. 2002). It is evident that the vector wind component fluctuations are neither independent nor Gaussian: the variance of  $V$  is greater for  $U > 0$  than it is for  $U < 0$ , and the marginal PDF of  $U$  is positively skewed and bimodal with peaks at about  $\pm 5 \text{ m s}^{-1}$  [although this bimodality may be an artifact resulting from the minima in  $p(U, V)$  around  $(0, 0) \text{ m s}^{-1}$ ]. In fact, the joint PDF of  $U$  and  $V$  is suggestive of two statistical populations: a first characterized by relatively weak fluctuations, with  $U < 0$  on average, and a second with stronger fluctuations and  $U > 0$  on average. These populations correspond to the easterly and westerly wind belts, respectively; the larger variance of  $V$  for

$U > 0$  than for  $U < 0$  evident in Fig. 7 simply reflects the fact that the storm tracks occur in the westerlies.

The right-hand panel of Fig. 7 displays both the observed PDF of  $w$  and the Weibull distribution with  $b = 2$  (so the distribution is Rayleigh) and  $a = \text{mean}(w)/\Gamma(3/2)$  {an essentially identical PDF is obtained using Eq. (5) with  $\sigma^2 = [\text{std}^2(U) + \text{std}^2(V)]/2$ }. The observed PDF of  $w$  is somewhat narrower than the Rayleigh PDF, with a somewhat larger most likely wind speed ( $7 \text{ m s}^{-1}$  in contrast to  $6.5 \text{ m s}^{-1}$  for the Rayleigh distribution). Despite these small differences, the Rayleigh PDF is a reasonable approximation to the global PDF of  $w$ .

Non-Rayleigh structure in the global PDF of  $w$  can arise due to violations of any of the assumptions, described above, from which the Rayleigh distribution follows rigorously. First, it is evident that the marginal distributions of  $U$  and  $V$  are non-Gaussian. Second, although the vector winds are uncorrelated (the correlation coefficient is  $-0.02$ ), they are not independent, as easterly winds are associated with smaller variability in  $v$  than are westerlies. Note that the independence of two variables always implies a vanishing correlation coefficient, but not vice versa; the correlation coefficient is only a linear measure of dependence. For example, a normal random variable  $x$  with zero mean and unit variance is uncorrelated with the variable  $y = x^2$ , but the two are clearly not independent. Statistical independence of two variables  $x$  and  $y$  requires that their joint PDF  $p(x, y)$  factor as the product  $p(x)p(y)$ , where  $p(x)$  and  $p(y)$  are the marginal distributions of  $x$  and  $y$ , and  $p(U, V)$  does not factor as  $p(U)p(V)$ . Direct calculation yields  $\text{mean}(U) = 0.21 \text{ m s}^{-1}$  and  $\text{mean}(V) = 0.13 \text{ m s}^{-1}$ , as well as  $\text{std}(U) = 6.7 \text{ m s}^{-1}$  and  $\text{std}(V) = 5.6 \text{ m s}^{-1}$ . The means of the vector wind components are an order of magnitude smaller than their standard deviations, so the assumption of a zero mean vector wind is reasonable. However, as typical fluctuations in the zonal wind are 20% larger than typical fluctuations in the meridional wind, the assumption of isotropy is violated. Non-Rayleigh behavior in the global PDF of  $w$  may arise, then, from non-Gaussian structure in the PDFs of the zonal and meridional winds, from statistical dependence between  $U$  and  $V$ , or from nonisotropic fluctuations in the vector wind.

## 6. Wind speed PDFs: Stochastic boundary layer model

To obtain a physical understanding of the observed PDFs of sea surface wind speeds, we will consider the simple stochastic model for boundary layer winds introduced in Monahan (2004b). This model has been

demonstrated to be useful in understanding observed relationships between moments of the sea surface vector winds (Monahan 2004a,b) and is in good qualitative agreement with empirical stochastic models of sea surface winds (Sura 2003; Sura and Sardeshmukh 2004, manuscript submitted to *J. Atmos. Sci.*, hereafter SS04). At any given location over the sea surface, we will define the surface wind vector components relative to a local coordinate system:

$$\begin{aligned} u &= \text{wind component along local mean wind vector,} \\ v &= \text{wind component across local mean wind} \\ &\quad \text{vector (positive to the left).} \end{aligned}$$

Denoting the vector wind by  $\mathbf{u} = (u, v)$ , the eddy-averaged horizontal momentum equation can be written

$$\frac{\partial \mathbf{u}}{\partial t} + \mathbf{u} \cdot \nabla \mathbf{u} = -\frac{1}{\rho} \nabla p - f \hat{\mathbf{k}} \times \mathbf{u} - \frac{1}{\rho} \frac{\partial (\rho \overline{\mathbf{u}'u'_3})}{\partial z}, \quad (18)$$

where  $p$  is the pressure,  $\rho$  is the air density,  $f$  is the Coriolis parameter, and  $u_3$  is the vertical velocity component. An analytically tractable model can be obtained as follows. First, Eq. (18) is integrated from the surface  $z = 0$  to an altitude  $z = h$  in the mixed layer. Second, horizontal advection of momentum is neglected; that is, a “single-column model” approximation is made. Third, the surface eddy momentum flux is represented in terms of a standard Monin–Obukhov bulk parameterization with drag coefficient  $c_d$ . Finally, the eddy momentum flux from above  $z = h$  is expressed in terms of a “finite-differenced” eddy flux:

$$\overline{\mathbf{u}'u'_3} = -\frac{K}{h} (\mathbf{U} - \mathbf{u}), \quad (19)$$

where  $K$  is a kinematic eddy viscosity and  $\mathbf{U}$  represents the wind vector above  $z = h$ . The resulting differential equation can be expressed as

$$\frac{d\mathbf{u}}{dt} = \mathbf{\Pi} - \frac{c_d}{h} w \mathbf{u} - \frac{K}{h^2} \mathbf{u}, \quad (20)$$

where we have defined the quantity

$$\mathbf{\Pi} = -\frac{1}{\rho} \nabla p - f \hat{\mathbf{k}} \times \mathbf{u} + \frac{K}{h^2} \mathbf{U}. \quad (21)$$

For the sake of convenience, we will assume that  $\mathbf{\Pi}$  does not depend on  $\mathbf{u}$ ; in particular, we assume that the ageostrophic residual between the pressure gradient force and the Coriolis force does not depend on the wind vector  $\mathbf{u}$ . Away from the equator, this approximation is similar to a small Rossby number approximation. Finally, we will assume that the forcing  $\mathbf{\Pi}$  is fluctuating around some mean value:

$$\Pi_u(t) = \langle \Pi_u \rangle + \Sigma \dot{W}_1(t), \quad (22)$$

$$\Pi_v(t) = \Sigma \dot{W}_2(t), \quad (23)$$

where the fluctuations are taken to be isotropic and white in time:

$$\langle \dot{W}_i(t_1) \dot{W}_j(t_2) \rangle = \delta_{ij} \delta(t_1 - t_2) \quad (24)$$

(where angle brackets denote ensemble averaging), with a strength that is tuned by the parameter  $\Sigma$ . Note that as by definition the average cross-mean wind is zero, so the average of  $\Pi_v$  must also be zero. The resulting equations for  $u$  and  $v$  read

$$\dot{u} = \langle \Pi_u \rangle - \frac{c_d}{h} w u - \frac{K}{h^2} u + \Sigma \dot{W}_1, \quad (25)$$

$$\dot{v} = -\frac{c_d}{h} w v - \frac{K}{h^2} v + \Sigma \dot{W}_2. \quad (26)$$

Equations (25)–(26) are a stochastic differential equation (SDE) for the surface wind vector; an introduction to SDEs can be found in Penland (2003a,b). The surface drag force depends on the wind speed  $w = \sqrt{u^2 + v^2}$ , the depth  $h$  of the atmospheric layer considered [taken as in Monahan (2004b) to be 80 m], and the drag coefficient  $c_d$ . In general, nonneutral stratification of the boundary layer and modification of the local sea state by surface winds both result in a dependence of  $c_d$  on  $w$  (through the Obukhov length in the first instance and the roughness length in the second). Furthermore, other factors such as surface surfactants and remotely generated swell introduce variations in the drag coefficient that are unrelated to the local winds. For simplicity, we will neglect the effects of stratification and swell and consider the parameterization of the neutral drag coefficient for fully developed seas introduced by Taylor and Yelland (2001), as modified in Fairall et al. (2003) to include a correction for flow over an aerodynamically smooth surface during conditions of light winds. The drag coefficient is determined by the surface roughness length  $z_0$  through

$$c_d = \frac{\kappa^2}{[\ln(10m/z_0)]^2}, \quad (27)$$

where  $\kappa = 0.4$  is von Kármán's constant and

$$z_0 = (4.11 \times 10^{-6} \text{s}^2 \text{m}^{-1}) w^2 + \frac{0.11 \nu}{\sqrt{c_d w}}, \quad (28)$$

with  $\nu$  the kinematic viscosity of water. In the Taylor and Yelland (2001) parameterization, the roughness length depends on the significant wave height and dominant wave period, both of which are taken to depend on local wind speed; these dependences are combined

to yield the first term on the right-hand side of Eq. (28). Note that as the roughness length depends explicitly on the drag coefficient, Eqs. (27) and (28) must be solved iteratively. The dependence of the neutral drag coefficient on the surface wind speed remains a subject of active research (e.g., Jones and Toba 2001; Fairall et al. 2003), and questions remain as to its precise formulation. Calculations using different expressions for the wind speed dependence of the drag coefficient (not shown) demonstrate that the following results are not qualitatively sensitive to which of the various parameterizations of  $c_d$  suggested in the literature are used.

One of Einstein's major insights in his *annus mirabilis* (Einstein 1956) was that the PDF of the solutions of an SDE satisfies a diffusion equation that has come to be referred to as a Fokker–Planck equation (e.g., Gardiner 1997; Penland 2003a,b). In particular, the stationary joint PDF of  $u$  and  $v$ ,  $p(u, v)$ , associated with the SDEs (25)–(26) satisfies the Fokker–Planck equation:

$$0 = \frac{\partial}{\partial u} \left( \langle \Pi_u \rangle - \frac{c_d}{h} w u - \frac{K}{h^2} u \right) p + \frac{\partial}{\partial v} \left( -\frac{c_d}{h} w v - \frac{K}{h^2} v \right) p + \frac{\Sigma^2}{2} \left( \frac{\partial^2 p}{\partial u^2} + \frac{\partial^2 p}{\partial v^2} \right), \quad (29)$$

which has the solution

$$p(u, v) = \mathcal{N}_G \exp \left( \frac{2}{\Sigma^2} \left\{ \langle \Pi_u \rangle u - \frac{K}{2h^2} (u^2 + v^2) - \frac{1}{h} \int_0^{\sqrt{u^2+v^2}} c_d(w') w'^2 dw' \right\} \right), \quad (30)$$

where  $\mathcal{N}_G$  is a normalization constant. Note that the PDF Eq. (30) is symmetric in  $v$ , so

$$\int_{-\infty}^{\infty} \int_{-\infty}^{\infty} u v p(u, v) du dv = 0. \quad (31)$$

Fluctuations in  $u$  and  $v$  are therefore uncorrelated, although they are not independent [i.e.,  $p(u, v)$  does not factor as the product of the marginal distributions of  $u$  and  $v$ ]. Independence of  $u$  and  $v$  holds only in the unphysical case of linear surface drag,  $c_d = k/w$ . An analytic expression for the PDF of  $w$  can be obtained from Eq. (30) as follows: moving to polar coordinates

$$u = w \cos \theta, \quad \text{and} \quad (32)$$

$$v = w \sin \theta; \quad (33)$$

such that the average value of  $\theta$  is zero (by construction), conservation of probability under a coordinate change requires that the joint PDF  $p(w, \theta)$  must satisfy

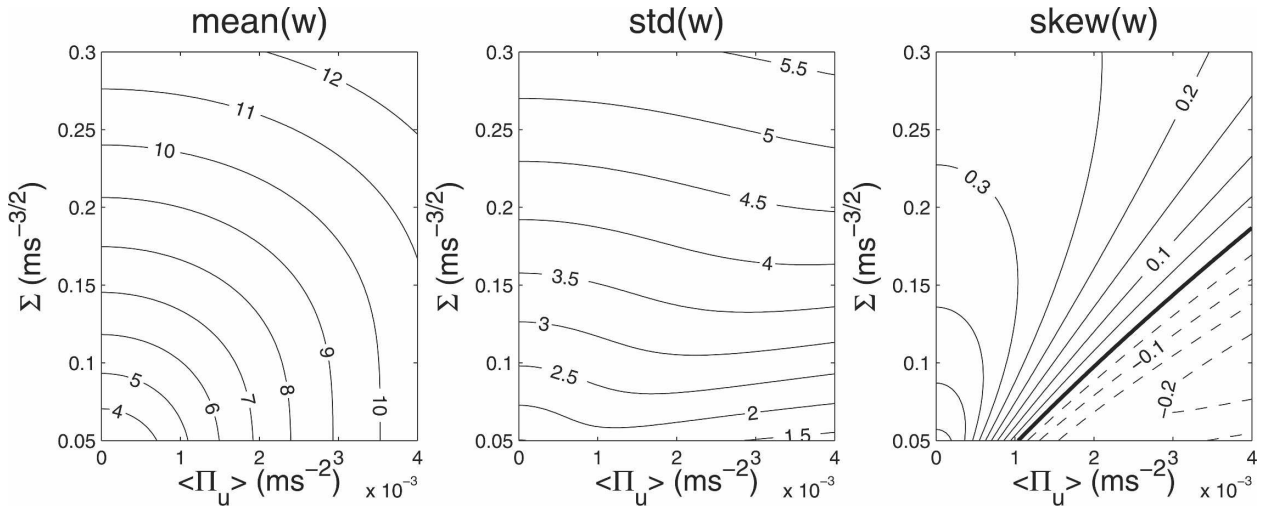


FIG. 8. Predicted mean, std dev, and skewness of wind speed  $w$  from the PDF Eq. (37), contoured as functions of the mean forcing  $\langle \Pi_u \rangle$  and fluctuation strength  $\Sigma$ .

$$\begin{aligned}
 p(u, v) du dv &= p(w \cos\theta, w \sin\theta) w dw d\theta \\
 &= p(w, \theta) dw d\theta.
 \end{aligned}
 \tag{34}$$

Thus,

$$\begin{aligned}
 p(w, \theta) &= \mathcal{N}_1 w \exp\left(\frac{2}{\Sigma^2} \left\{ \langle \Pi_u \rangle w \cos\theta - \frac{K}{2h^2} w^2 \right. \right. \\
 &\quad \left. \left. - \frac{1}{h} \int_0^w c_d(w') w'^2 dw' \right\}\right).
 \end{aligned}
 \tag{35}$$

The marginal distribution  $p(w)$  for the wind speed  $w$  is obtained by integrating  $p(w, \theta)$  over the angle  $\theta$ . An analytic expression for this integral follows from the fact that (for  $n$  an integer)

$$I_n(z) = \frac{1}{2\pi} \int_0^{2\pi} d\theta \exp(z \cos\theta) \cos n\theta,
 \tag{36}$$

where  $I_n$  is the modified Bessel function of order  $n$  (Abramowitz and Stegun 1972). Performing the integral, we obtain the closed-form expression:

$$\begin{aligned}
 p(w) &= \mathcal{N}_1 w I_0\left(\frac{2\langle \Pi_u \rangle w}{\Sigma^2}\right) \exp\left\{-\frac{2}{\Sigma^2} \left[ \frac{K}{2h^2} w^2 \right. \right. \\
 &\quad \left. \left. + \frac{1}{h} \int_0^w c_d(w') w'^2 dw' \right] \right\}.
 \end{aligned}
 \tag{37}$$

The mean, standard deviation, and skewness of wind speed  $w$  from Eq. (37) are contoured as functions of  $\langle \Pi_u \rangle$  and  $\Sigma$  in Fig. 8; the ranges of these parameters were chosen so that the ranges of the simulated moments were quantitatively similar to those observed

(Fig. 2). A typical boundary layer value of  $K = 1 \text{ m}^2 \text{ s}^{-1}$  was used. The mean wind speed is an increasing function of both  $\langle \Pi_u \rangle$  and  $\Sigma$ . The standard deviation of  $w$  is determined primarily by  $\Sigma$ , displaying only a weak dependence on  $\langle \Pi_u \rangle$ . Finally, skewness of  $w$  depends on both  $\langle \Pi_u \rangle$  and  $\Sigma$ ; in particular, the skewness of  $w$  is negative when the forcing has a large mean but relatively small fluctuations; as the magnitude of the fluctuations increases, the skewness eventually becomes positive.

Inspection of Fig. 2 indicates that in general the surface wind speed distribution is negatively skewed in the eastern equatorial Pacific and along the equatorward flanks of the subtropical highs, regions characterized by relatively high mean wind speeds and relatively low variability. The regions of strongest positive skewness are the Northern Hemisphere midlatitudes, characterized by intermediate mean wind speeds and strong variability. Finally, the Southern Ocean is characterized by high mean( $w$ ), intermediate std( $w$ ), and skew( $w$ ) close to zero. Qualitatively, the relationship between the spatial structures of the mean( $w$ ), std( $w$ ), and skew( $w$ ) fields is as predicted by the PDF Eq. (37).

The agreement of the relationships between moments from the observations and from the PDF Eq. (37) is most obvious in a plot of skew( $w$ ) as a function of mean( $w$ )/std( $w$ ) (Fig. 9). Values of mean( $w$ ), std( $w$ ), and skew( $w$ ) for the PDF Eq. (37) were sampled on a regular grid of the parameters  $\langle \Pi_u \rangle$  and  $\Sigma$  over the range of values displayed in Fig. 8; although skew( $w$ ) is not exactly a single-valued function of the ratio mean( $w$ )/std( $w$ ), its values cluster tightly around a one-dimensional curve. Like the associated curve for a

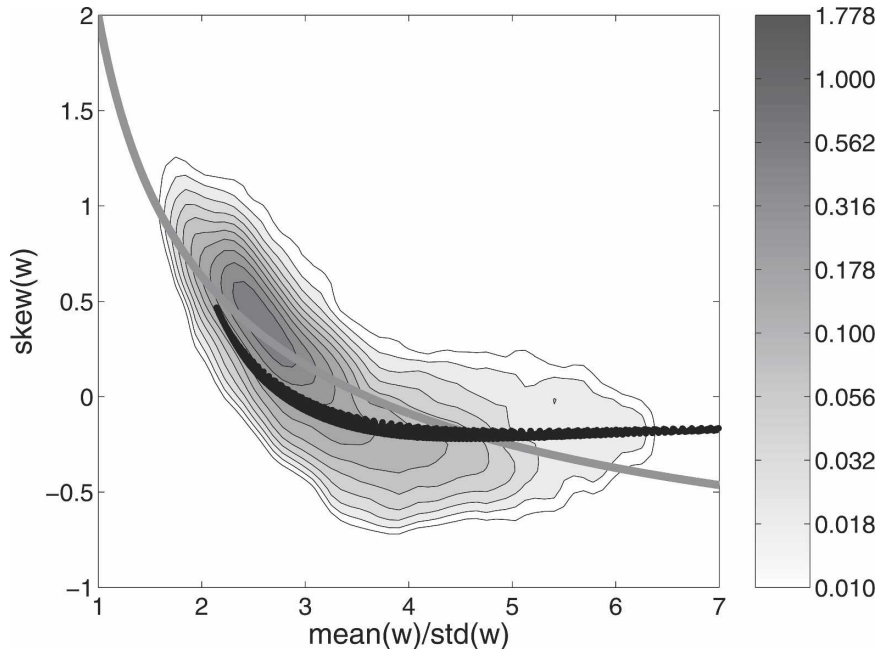


FIG. 9. Plots of the relationship between  $\text{mean}(w)/\text{std}(w)$  and  $\text{skew}(w)$  for a Weibull distribution [Eqs. (8)–(10), gray line] and for the theoretical PDF Eq. (37) (black line), superimposed on the kernel density estimate of the joint PDF of  $\text{mean}(w)/\text{std}(w)$  and  $\text{skew}(w)$  from SeaWinds observations (contoured on a logarithmic scale).

Weibull distribution, this curve is concave upward and runs through the middle of the observed joint PDF of  $\text{mean}(w)/\text{std}(w)$  and  $\text{skew}(w)$ , taking positive values when the ratio  $\text{mean}(w)/\text{std}(w)$  is small and negative values when this ratio is large. In fact, for values of this ratio of approximately 2 and greater, the curve predicted by the stochastic boundary layer model is at least as good a representation of the observed joint PDF as is the Weibull curve. For lower values of the ratio, however, the performance of the model is not so good: the predicted skewness does not take values greater than approximately 0.5, considerably below the maximum observed skewness. It is evident that while both the Weibull distribution and the PDF Eq. (37) capture aspects of the relationships between moments observed in sea surface wind speeds, neither is entirely accurate. It should be emphasized, however, that the PDF Eq. (37) arises from physical arguments with a clear series of approximations, while the Weibull characterization of sea surface wind speeds is entirely empirical. The success of the Weibull distribution as a useful approximation to the distribution of  $w$  evidently arises because it imposes the constraints on the relationship between  $\text{mean}(w)$ ,  $\text{std}(w)$ , and  $\text{skew}(w)$  that are required by the physics of the atmospheric boundary layer.

An intuitive understanding of the dependence of  $\text{mean}(w)$ ,  $\text{std}(w)$ , and  $\text{skew}(w)$  on  $\langle \Pi_u \rangle$  and  $\Sigma$  is straight-

forward. An increase in  $\langle \Pi_u \rangle$  will lead to an increase in  $\text{mean}(u)$ , and consequently to an increase in the mean wind speed. The joint PDF of  $u$  and  $v$  becomes broader as  $\Sigma$  increases; this shift of probability mass away from the origin increases both the mean amplitude  $w$  of the vector wind and its variability. Finally, the skewness of  $w$  is determined by the width of the PDF of  $w$  relative to its mean value, that is, the ratio  $\text{mean}(w)/\text{std}(w)$ . For smaller values of this ratio, the distribution  $p(u, v)$  is concentrated around the origin, and the distribution of the magnitude  $w$  has a tail toward larger values, so  $\text{skew}(w)$  is positive. Conversely, for larger values of this ratio, the joint PDF  $p(u, v)$  is centered away from the origin. Because of the anticorrelation of  $\text{mean}(u)$  and  $\text{skew}(u)$  discussed in Monahan (2004a, b),  $p(u, v)$  will be characterized by a tail extending toward the origin. As the mass of  $p(u, v)$  is concentrated away from the origin, this tail will also be present in the marginal PDF of  $w$ , so  $\text{skew}(w)$  will be negative. The fact that the PDF Eq. (37) can become negatively skewed is a consequence of the anticorrelation between the mean and skewness of the vector wind components, which can be understood to arise because of the nonlinearity of the surface drag law. For a linear drag law ( $c_d = k/w$ ), for which the vector winds are Gaussian, the skewness of  $w$  from PDF Eq. (37) (not shown) is always positive.

## 7. Wind speed PDFs: Empirical parameterization

While the stochastic boundary layer model [Eqs. (25)–(26)] provides physical insight into the PDF of sea surface wind speeds, it is too simple to be quantitatively accurate. In particular, the range of values of skew( $w$ ) from the PDF Eq. (37) is considerably smaller than the observed range (Fig. 9). Furthermore, the quantities  $\langle \Pi_u \rangle$  and  $\Sigma$  are difficult to obtain from observations. To obtain a more useful and more quantitatively accurate expression for  $p(w)$ , we will consider another approach, extending an analysis presented in CMT. This earlier study assumed that  $u$  and  $v$  were independent and Gaussian with isotropic fluctuations, but in contrast to the argument leading to the PDF Eq. (5) the mean vector wind was *not* assumed to be zero. The distributions of  $u$  and  $v$  are thus

$$p(u) = \frac{1}{\sqrt{2\pi\sigma^2}} \exp\left[-\frac{(u - \bar{u})^2}{2\sigma^2}\right], \quad (38)$$

$$p(v) = \frac{1}{\sqrt{2\pi\sigma^2}} \exp\left(-\frac{v^2}{2\sigma^2}\right), \quad (39)$$

where  $\bar{u}$  is the magnitude of the average vector wind and  $\sigma$  is the standard deviation of both  $u$  and  $v$ . The assumption of independence implies that the joint PDF of  $u$  and  $v$  is the product of their marginal distributions:

$$p(u, v) = \frac{1}{2\pi\sigma^2} \exp\left(-\frac{(u - \bar{u})^2 + v^2}{2\sigma^2}\right), \quad (40)$$

so

$$p(w, \theta) = \frac{w}{2\pi\sigma^2} \exp\left(-\frac{1}{2\sigma^2}(w^2 + \bar{u}^2)\right) \exp\left(\frac{w\bar{u}}{\sigma^2} \cos\theta\right) \quad (41)$$

and, integrating over  $\theta$ ,

$$p(w) = I_0\left(\frac{w\bar{u}}{\sigma^2}\right) \frac{w}{\sigma^2} \exp\left[-\frac{1}{2\sigma^2}(w^2 + \bar{u}^2)\right]. \quad (42)$$

We will refer to the PDF Eq. (42) as the CMT distribution (CMT); note that the PDF of the scalar wind speed  $w$  has been expressed in terms of the average and variability of the vector wind. As discussed in CMT,  $p(w)$  reduces to the Rayleigh distribution Eq. (5) in the limit that  $\bar{u} \rightarrow 0$ , as would be expected. Furthermore, it is worth noting that the CMT distribution arises from the boundary layer model [Eqs. (25)–(26)] in the case of a linear surface drag ( $c_d = k/w$ ), with

$$\bar{u} = \langle \Pi_u \rangle \left( \frac{K}{h^2} + \frac{k}{h} \right)^{-1}, \quad (43)$$

$$\sigma = \left( \frac{2K}{h^2} + \frac{2k}{h} \right)^{-1/2} \Sigma. \quad (44)$$

To determine the accuracy of the CMT distribution in characterizing the probability distribution of sea surface wind speeds,  $\bar{u}$  and  $\sigma^2$  were estimated from the SeaWinds surface wind data. Because fluctuations in the along- and cross-mean wind directions are not exactly isotropic,  $\sigma$  was estimated as

$$\sigma = \left\{ \frac{1}{2} [\text{std}^2(u) + \text{std}^2(v)] \right\}^{1/2}. \quad (45)$$

The upper panels of Fig. 10 illustrate the mean, standard deviation, and skewness fields of the surface wind speed calculated from the CMT distribution using the observed  $\bar{u}$  and  $\sigma$  fields; these should be compared with the moment fields from observations presented in Fig. 2. Maps of the differences between the observed moment fields and those predicted by the CMT distribution are presented in Fig. 11. The CMT distribution generally underestimates mean( $w$ ) and overestimates std( $w$ ); differences are particularly large over the Southern Ocean, where predicted values of mean( $w$ ) can be greater than  $0.5 \text{ m s}^{-1}$  too low and of std( $w$ ) can be over  $1 \text{ m s}^{-1}$  too large. Furthermore, in both the subtropics and the Southern Hemisphere middle latitudes, the CMT distribution overestimates skew( $w$ ); in particular, the CMT distribution is unable to reproduce the negative skewnesses of  $w$  observed in the subtropics and the band of near-zero skewness over the Southern Ocean. It was argued in the previous section that these features of the wind speed skewness field can be understood to arise from the strong negative skewness of the along-mean wind component of the vector wind in these regions. As the skewness of the vector wind components is assumed to be zero in the derivation of the CMT distribution, it is not surprising that this distribution is unable to reproduce these features of the observed sea surface wind speed skewness field.

The derivation of the CMT distribution presented above can be extended to include non-Gaussian along-mean wind surface wind components as follows. As was pointed out in Thompson et al. (1983), the distribution

$$p(u) = \frac{1}{\sqrt{2\pi\sigma^2}} \left[ 1 + \frac{\nu}{6} \text{He}_3\left(\frac{u - \bar{u}}{\sigma}\right) \right] \times \exp\left[-\frac{(u - \bar{u})^2}{2\sigma^2}\right] \quad (46)$$

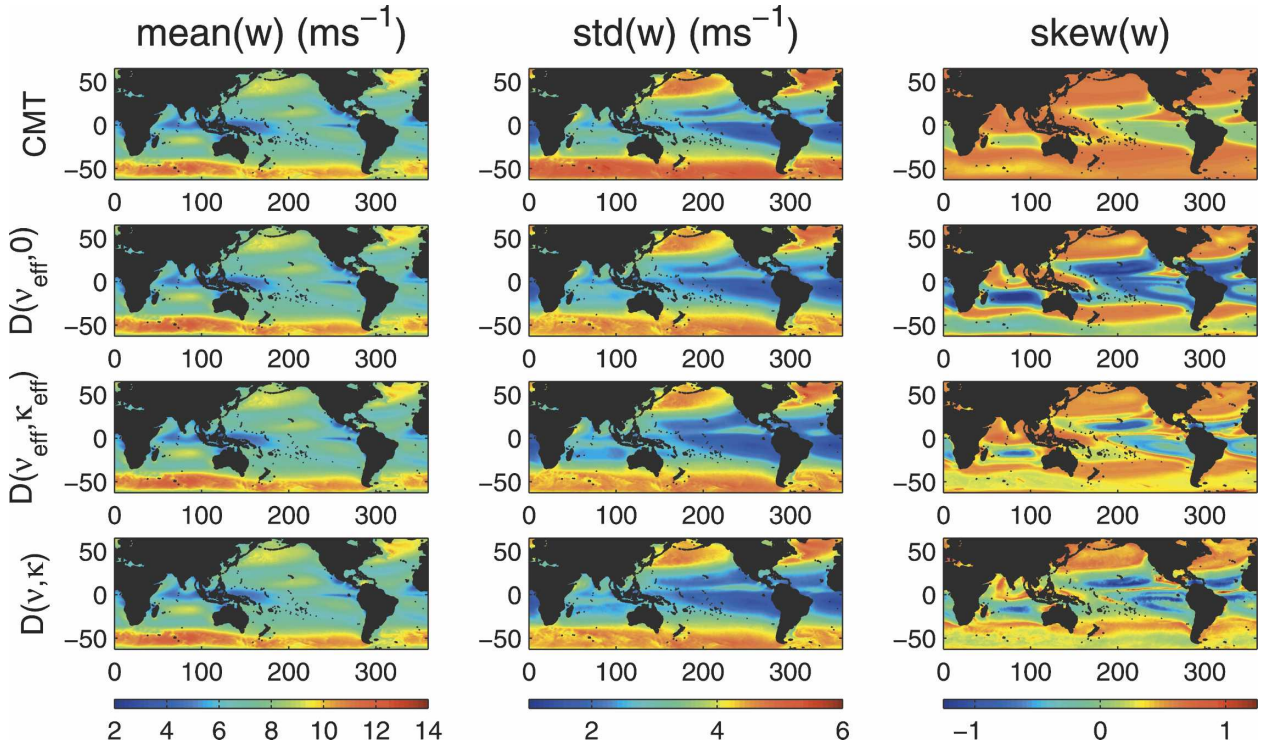


FIG. 10. Mean, std dev, and skewness of  $w$  from CMT,  $D(v_{\text{eff}}, 0)$ ,  $D(v_{\text{eff}}, \kappa_{\text{eff}})$ , and  $D(v, \kappa)$  distributions.

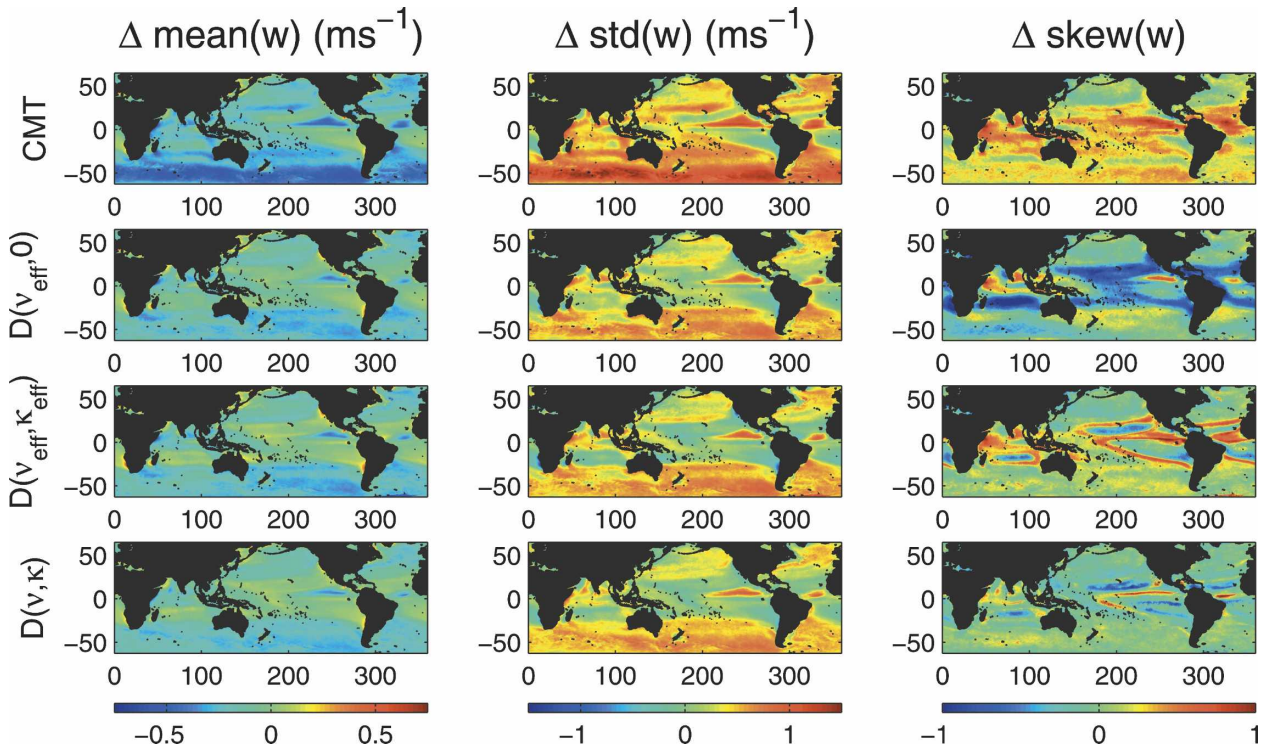


FIG. 11. Same as in Fig. 10, but for predicted moments of  $w$  minus the observed moments.

will have mean  $\bar{u}$ , standard deviation  $\sigma$ , and skewness  $\nu$ , where

$$\text{He}_3(x) = x^3 - 3x \quad (47)$$

is the Hermite polynomial of order 3 [following the notation of Gradshteyn and Ryzhik (2000, p. xxxvii)]. The distribution Eq. (46) is a low-order Gram–Charlier expansion (Johnson et al. 1994) of the Gaussian PDF Eq. (38). A drawback with the Gram–Charlier expansion of a PDF is that the resulting distribution is not guaranteed to be positive definite: negative values of the distribution can occur, so that it is no longer a PDF

in strict terms. Algorithms exist to impose the constraint of nonnegativity on Gram–Charlier distributions (e.g., Jondeau and Rockinger 2001) at the expense of an analytic expression for the density. In practice, we find that the Gram–Charlier densities only ever become slightly negative for the parameter values used in the present analysis.

Proceeding as with the derivation of the CMT distribution, assuming independent, isotropic fluctuations in  $u$  and  $v$ , but using the skewed Gram–Charlier distribution of  $u$  Eq. (46) instead of the Gaussian distribution Eq. (38), after integrating over the angle  $\theta$  we arrive at the marginal distribution for the wind speed  $w$ :

$$p(w) = \frac{w}{\sigma^2} \exp\left(-\frac{w^2 + \bar{u}^2}{2\sigma^2}\right) \left\{ \left[ 1 - \frac{\nu}{6} \text{He}_3\left(\frac{\bar{u}}{\sigma}\right) \right] I_0\left(\frac{w\bar{u}}{\sigma^2}\right) + \frac{\nu}{2} \left(\frac{w}{\sigma}\right) \text{He}_2\left(\frac{\bar{u}}{\sigma}\right) I_1\left(\frac{w\bar{u}}{\sigma^2}\right) - \frac{\nu}{4} \left(\frac{w}{\sigma}\right)^2 \left(\frac{\bar{u}}{\sigma}\right) \left[ I_0\left(\frac{w\bar{u}}{\sigma^2}\right) + I_2\left(\frac{w\bar{u}}{\sigma^2}\right) \right] + \frac{\nu}{24} \left(\frac{w}{\sigma}\right)^3 \left[ 3I_1\left(\frac{w\bar{u}}{\sigma^2}\right) + I_3\left(\frac{w\bar{u}}{\sigma^2}\right) \right] \right\}, \quad (48)$$

where

$$\text{He}_2(x) = x^2 - 1 \quad (49)$$

is the second-order Hermite polynomial. The PDF Eq. (48) will be denoted the  $D(\nu, 0)$  distribution.

The spatial anticorrelation between mean( $u$ ) and skew( $u$ ) discussed in Monahan (2004b) suggests that a parameterization can be developed in which the higher-order moment is obtained from the lower-order moment. Such a parameterization will allow the  $D(\nu, 0)$  distribution to be evaluated with no more input data than is required by the CMT distribution. In fact, as discussed in Monahan (2004a) and Monahan (2004b), skew( $u$ ) depends (nonlinearly) on std( $u$ ) as well. Because we are interested in developing a parameterization of skew( $u$ ) for use in Eq. (48), we will look for a model of the form

$$\text{skew}(u) = \nu_{\text{eff}}(\bar{u}, \sigma) + \varepsilon, \quad (50)$$

where  $\varepsilon$  is some residual. Ideally, such a parameterization would be derived from a mechanistic model such as Eqs. (25)–(26); this model, however, is too simple to be sufficiently quantitatively accurate for this purpose. We will instead estimate  $\nu_{\text{eff}}$  statistically from the observed moments of  $u$ . Because  $\nu_{\text{eff}}$  is expected to be a significantly nonlinear function of  $\bar{u}$  and  $\sigma$ , it is estimated using a standard feed-forward neural network (e.g., Hsieh and Tang 1998) with five “hidden neurons.” Neural networks are a flexible tool for nonparametric, non-

linear function estimation; for the present application, the statistical models fit to the neural network were found to outperform polynomial nonlinear regression models with a similar number of parameters (not shown). The left panels of Fig. 12 display maps of the skewness fields of  $u$  from observations and from the best-fit model Eq. (50). While the neural network model generally underestimates the extremes of the observed skewness field, it is generally successful in capturing the spatial structure of the observed field.

Maps of mean( $w$ ), std( $w$ ), and skew( $w$ ) predicted by the  $D(\nu_{\text{eff}}, 0)$  distribution obtained using the empirical skewness field  $\nu_{\text{eff}}$  are presented in the second row of Fig. 10; the associated difference maps are presented in Fig. 11. Similarly to the CMT distribution, the  $D(\nu_{\text{eff}}, 0)$  distribution underestimates mean( $u$ ) and overestimates std( $u$ ) in the midlatitudes. However, the absolute errors are generally considerably smaller (by 40% on average) for the  $D(\nu_{\text{eff}}, 0)$  distribution than for the CMT distribution. Furthermore, unlike the CMT distribution, the  $D(\nu_{\text{eff}}, 0)$  distribution is able to capture the negative skewness of  $w$  in the subtropics and the band of near-zero skewness around the Southern Ocean. However, the subtropical negative skewness of  $w$  is overestimated by  $D(\nu_{\text{eff}}, 0)$ , leading to a strong negative bias in skew( $w$ ) in the subtropics of both hemispheres, and a slight positive bias in skew( $w$ ) is evident in the midlatitudes of the Southern Hemisphere. While the  $D(\nu_{\text{eff}}, 0)$  distribution improves considerably over the CMT distribution in its characterization of the leading moments of  $w$ , considerable biases remain.

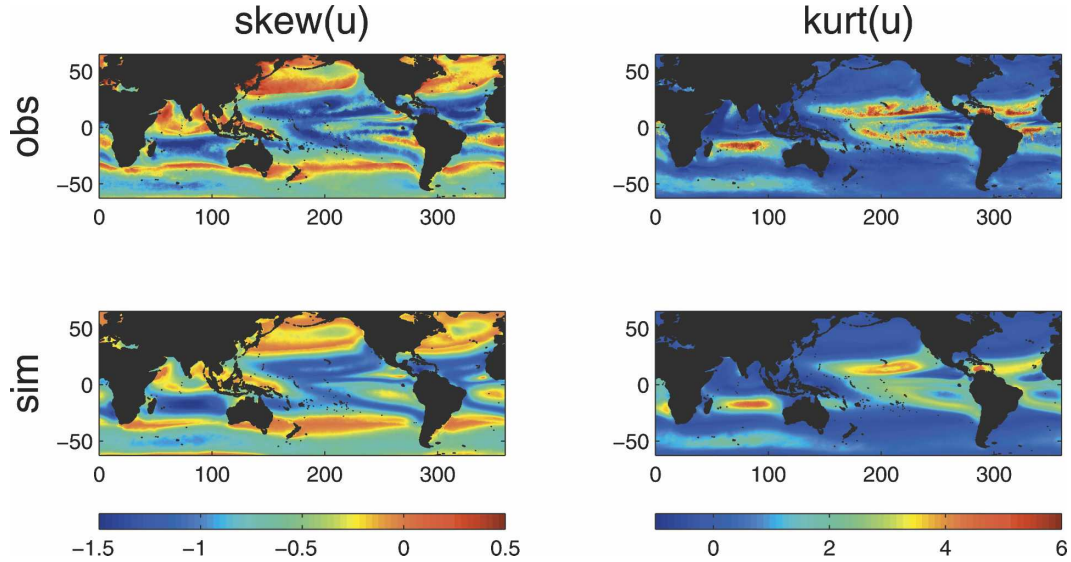


FIG. 12. Skewness and kurtosis of along-mean wind component  $u$  (top) from observations and (bottom) as simulated by the effective neural-network parameterizations  $\nu_{\text{eff}}$  [Eq. (50)] and  $\kappa_{\text{eff}}$  [Eq. (55)].

The characterization of the probability distribution of sea surface wind speed can be further improved by including the kurtosis of the along-mean wind surface vector wind component in the parameterization. As with the skewness, the kurtosis of  $u$  is also generally nonzero; the spatial distribution of  $\text{kurt}(u)$  is presented in Fig. 12. The kurtosis of  $u$  is between  $-1$  and  $1$  throughout most of the midlatitudes, increasing up to a value of  $2$  in the Atlantic–Indian Ocean sector of the Southern Ocean in which  $\text{mean}(u)$  is largest. Throughout the Tropics, the kurtosis is generally positive, taking values in excess of  $4$  in the central tropical Pacific (although the statistical significance of these large values is questionable). If the kurtosis of  $u$  is known, it can be included in an extended Gram–Charlier expansion of the Gaussian PDF Eq. (38); the distribution

$$p(u) = \frac{1}{\sqrt{2\pi\sigma^2}} \left[ 1 + \frac{\nu}{6} \text{He}_3\left(\frac{u - \bar{u}}{\sigma}\right) + \frac{\kappa}{24} \text{He}_4\left(\frac{u - \bar{u}}{\sigma}\right) \right] \exp\left(-\frac{(u - \bar{u})^2}{2\sigma^2}\right), \quad (51)$$

where

$$\text{He}_4(x) = x^4 - 6x^2 + 3 \quad (52)$$

is the fourth-order Hermite polynomial, will have specified mean  $\bar{u}$ , standard deviation  $\sigma$ , skewness  $\nu$ , and kurtosis  $\kappa$ . Again assuming isotropic and independent fluctuations in  $u$  and  $v$ , we obtain the following expression for the probability distribution of  $w$ :

$$p(w) = \left\{ \left[ 1 - \frac{\nu}{6} \text{He}_3\left(\frac{\bar{u}}{\sigma}\right) + \frac{\kappa}{24} \text{He}_4\left(\frac{\bar{u}}{\sigma}\right) \right] I_0\left(\frac{w\bar{u}}{\sigma^2}\right) + \frac{1}{2} \left(\frac{w}{\sigma}\right) \left[ \nu \text{He}_2\left(\frac{\bar{u}}{\sigma}\right) - \frac{\kappa}{3} \text{He}_3\left(\frac{\bar{u}}{\sigma}\right) \right] I_1\left(\frac{w\bar{u}}{\sigma^2}\right) + \frac{1}{8} \left(\frac{w}{\sigma}\right)^2 \left[ -2\nu \left(\frac{\bar{u}}{\sigma}\right) + \kappa \text{He}_2\left(\frac{\bar{u}}{\sigma}\right) \right] \left[ I_0\left(\frac{w\bar{u}}{\sigma^2}\right) + I_2\left(\frac{w\bar{u}}{\sigma^2}\right) \right] + \frac{1}{24} \left(\frac{w}{\sigma}\right)^3 \left[ \nu - \kappa \left(\frac{\bar{u}}{\sigma}\right) \right] \left[ 3I_1\left(\frac{w\bar{u}}{\sigma^2}\right) + I_3\left(\frac{w\bar{u}}{\sigma^2}\right) \right] + \frac{\kappa}{192} \left(\frac{w}{\sigma}\right)^4 \left[ 3I_0\left(\frac{w\bar{u}}{\sigma^2}\right) + 4I_2\left(\frac{w\bar{u}}{\sigma^2}\right) + I_4\left(\frac{w\bar{u}}{\sigma^2}\right) \right] \right\} \frac{w}{\sigma^2} \exp\left(-\frac{w^2 + \bar{u}^2}{2\sigma^2}\right). \quad (53)$$

This PDF will be denoted as  $D(\nu, \kappa)$ .

As was the case with  $\text{skew}(u)$ , observations and the boundary layer model [Eqs. (25)–(26)] indicate that

$\text{kurt}(u)$  is related to both  $\text{mean}(u)$  and  $\text{std}(u)$ . Joint PDFs of  $\text{mean}(u)$ ,  $\text{std}(u)$ , and  $\text{skew}(u)$  with  $\text{kurt}(u)$  from SeaWinds observations are presented in Fig. 13.

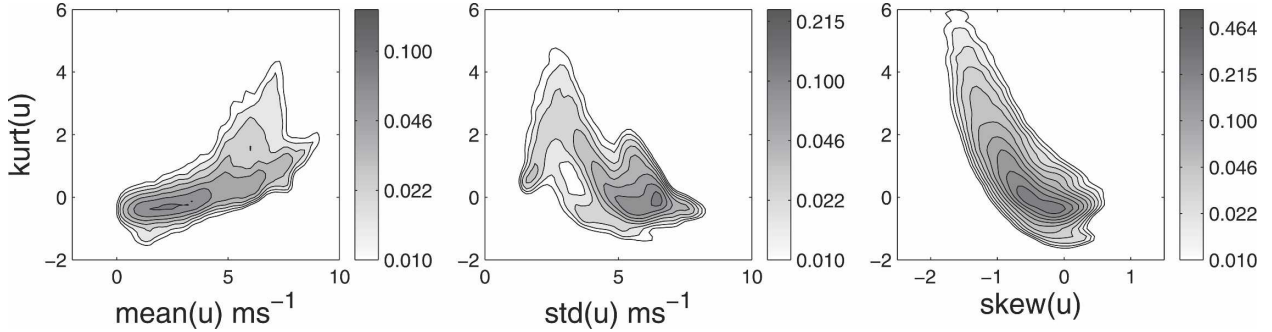


FIG. 13. Kernel density estimates (contoured on logarithmic scales) of joint PDFs of  $kurt(u)$  with  $mean(u)$ ,  $std(u)$ , and  $skew(u)$ .

Evidently,  $kurt(u)$  is generally negative for low  $mean(u)$  and increases as  $mean(u)$  increases;  $kurt(u)$  generally takes larger values for smaller values of  $std(u)$  and decreases as  $std(w)$  increases; and  $kurt(u)$  increases

with decreasing  $skew(u)$ . Contour plots of  $mean(u)$ ,  $std(u)$ ,  $skew(u)$ , and  $kurt(u)$  calculated from the marginal PDF for  $u$ ,

$$p(u) = \int_{-\infty}^{\infty} p(u, v) dv = \mathcal{N}_1 \exp\left(\frac{2\langle \Pi_u \rangle u}{\Sigma^2}\right) \int_{-\infty}^{\infty} \exp\left[-\frac{2}{\Sigma^2 h} \int_0^{\sqrt{u^2+v^2}} c_d(w') w'^2 dw'\right] dv, \quad (54)$$

are presented in Fig. 14. The first three of these plots agree well with similar plots for a simpler version of the model presented in Monahan (2004a). Although the boundary layer model considerably underestimates the values of  $kurt(w)$  compared to observations, the relationships between the observed moments evident in Fig. 13 are qualitatively consistent with those presented in Fig. 14: in general  $kurt(u)$  is an increasing function of  $mean(u)$  and a decreasing function of both  $std(u)$  and  $skew(u)$ .

In analogy with Eq. (50), we construct an empirical model

$$kurt(u) = \kappa_{eff}(\bar{u}, \sigma) + \varepsilon \quad (55)$$

using a feed-forward neural network. A map of  $\kappa_{eff}$  is presented in Fig. 12; it is broadly consistent with the observed kurtosis field, although it underestimates  $kurt(u)$  over the central Pacific and subtropical North Atlantic and Pacific Oceans.

Maps of  $mean(w)$ ,  $std(w)$ , and  $skew(w)$  calculated from the  $D(v_{eff}, \kappa_{eff})$  distribution are presented in the third row of Fig. 10; the corresponding maps of the difference with the observed moments appear in the third row of Fig. 11. Inclusion of information about the kurtosis of  $u$  does not significantly improve the representation of  $mean(w)$  or  $std(w)$  relative to the  $D(v_{eff}, 0)$  distribution, but the representation of  $skew(w)$  is considerably improved. The bands of negative bias in  $(w)$  characteristic of the  $D(v_{eff}, 0)$  distribution are largely eliminated in the  $D(v_{eff}, \kappa_{eff})$  distribution. Including in-

formation about the third- and fourth-order moments of the vector wind, parameterized in terms of the first and second moments, results in a representation of the PDF of sea surface wind speed that is a considerable improvement over the PDF arising from the assumption of Gaussian vector wind fluctuations. Note that the  $D(v_{eff}, \kappa_{eff})$  distribution does not make use of any more input information than does the CMT distribution.

Finally, differences are relatively small between the fields of  $mean(w)$ ,  $std(w)$ , and  $skew(w)$  predicted by the  $D(v_{eff}, \kappa_{eff})$  distribution and those predicted by the  $D(v, \kappa)$  distribution obtained using the observed  $skew(u)$  and  $kurt(u)$  fields in Eq. (53) (fourth row of Figs. 10 and 11). The  $D(v, \kappa)$  distribution represents the moments of  $w$  marginally better than the  $D(v_{eff}, \kappa_{eff})$  distribution but requires four pieces of information at each grid point  $(\bar{u}, \sigma, v, \kappa)$  rather than the two  $(\bar{u}, \sigma)$  required by  $D(v_{eff}, \kappa_{eff})$ .

It is noteworthy that particularly large biases in  $D(v, \kappa)$  occur where the assumptions of isotropic, independent fluctuations of the vector winds used to obtain Eq. (53) are most strongly violated. A map of the correlation coefficient between  $u$  and  $v$  is presented in the upper panel of Fig. 15, while the lower panel displays a map of the ratio of the standard deviations of  $u$  and  $v$  (a measure of anisotropy in fluctuations of the vector wind). In general, fluctuations in  $u$  and  $v$  are anisotropic and uncorrelated; notable exceptions occur in monsoon regions [the northern Indian Ocean and the eastern flanks of the subtropical anticyclones, e.g., Rodwell and

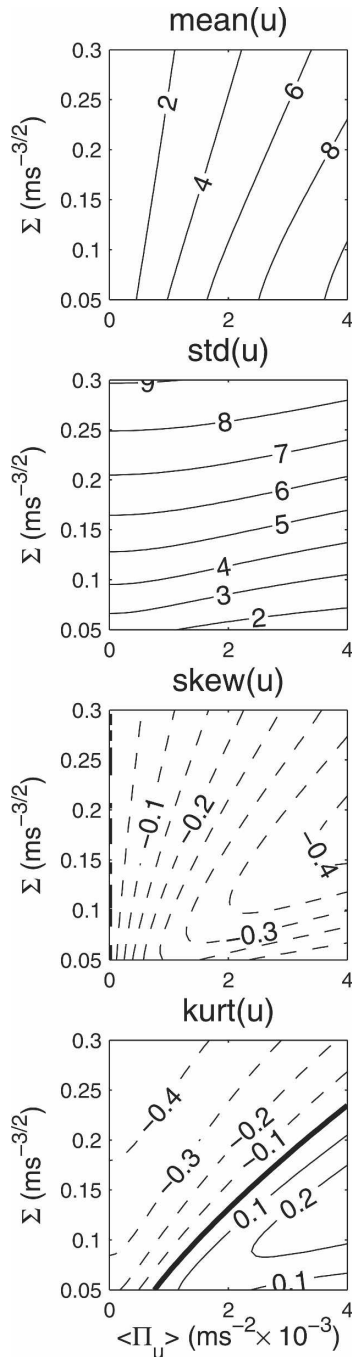


FIG. 14. Contour plots of  $\text{mean}(u)$ ,  $\text{std}(u)$ ,  $\text{skew}(u)$ , and  $\text{kurt}(u)$  as functions of  $\langle \Pi_u \rangle$  and  $\Sigma$  from the marginal PDF Eq. (54) derived from the stochastic boundary layer model [Eqs. (25)–(26)].

Hoskins (2001)] and the ITCZ and SPCZ. As well, fluctuations in  $u$  are slightly ( $\sim 20\%$ ) larger than those of  $v$  in the midlatitude storm tracks. Errors in  $\text{mean}(w)$  and  $\text{std}(w)$  for the distribution  $D(v, \kappa)$  are greatest in these regions where fluctuations in the vector wind are most correlated or anisotropic. A seasonally stratified analy-

sis of the correlation structure of the vector wind components (not shown) indicates that many of these correlated features (particularly in the Indian Ocean and along the equator) arise as a consequence of seasonal variability in the sea surface wind field.

Because of the nonlinear dependence on sea surface wind speed of bulk formulas for air–sea fluxes, the spatially or temporally averaged fluxes will not generally equal the fluxes associated with the average surface wind speed. In particular, grid-scale averages of these fluxes in general circulation models (GCMs) will not equal the fluxes associated with grid-scale winds. Furthermore, the average wind speed is not generally equal to the magnitude of the average vector wind: highly variable but isotropic fluctuations in the vector wind will be associated with a large average speed but yield a mean vector with small amplitude (e.g., Mahrt and Sun 1995; Levy and Vickers 1999). Improvements to calculations of the fluxes can be obtained through the use of parameterizations of the PDF of sea surface wind speed, which take as input grid-scale variables. The surface wind fields produced by GCMs represent grid-scale-averaged vector winds, but grid-scale wind speed distributions are required to diagnose air–sea fluxes. The distributions considered in this section provide a specification of the PDF of sea surface wind speeds from the mean and variance of the vector winds. The first of these quantities is a standard model field, while parameterizations of the second exist (e.g., CMT). The incorporation of these distributions into GCM calculations of air–sea fluxes is therefore straightforward in principle; an important and interesting extension of the present study would be an estimate of the effects on simulations of the climate system of including these distributions in the computation of air–sea fluxes.

## 8. Summary and conclusions

This study has considered the probability distribution of sea surface wind speeds ( $w$ ) observationally, using 6-yr worth of daily sea surface winds on a  $1/4^\circ \times 1/4^\circ$  grid from the SeaWinds scatterometer mounted on the NASA QuikSCAT satellite; theoretically, using a stochastic model derived using a clear sequence of approximations from the equations governing boundary layer physics; and empirically, using a class of models based on simplifying assumptions about the PDF of sea surface vector winds. The following results were obtained.

- Global fields of  $\text{mean}(w)$ ,  $\text{std}(w)$ , and  $\text{skew}(w)$  have been characterized, along with those of the Weibull scale and shape parameters  $a$  and  $b$ . When these

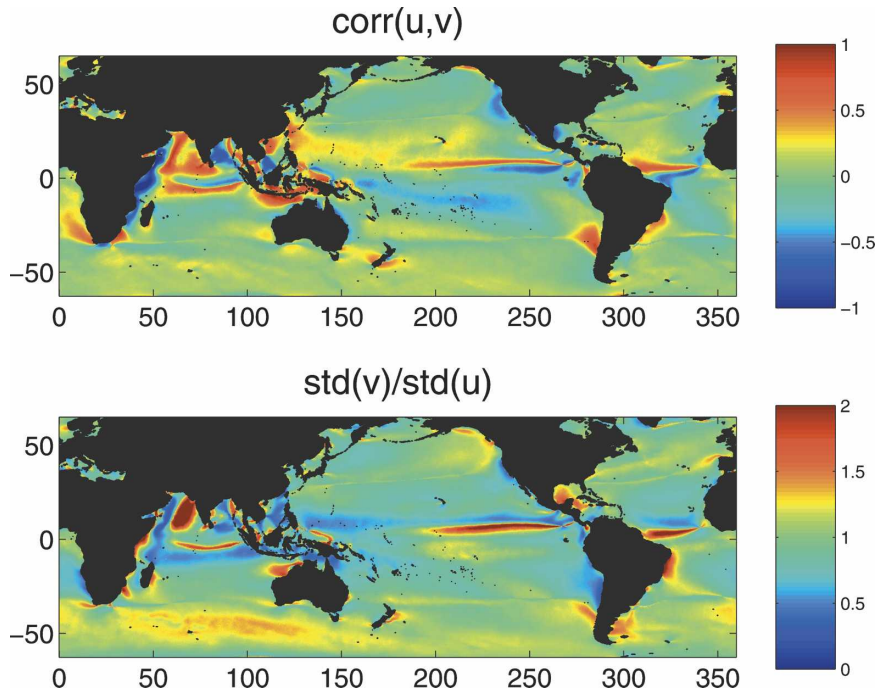


FIG. 15. (top) Map of the correlation coefficient between the along- and cross-mean wind surface wind components,  $u$  and  $v$ . (bottom) Map of the ratio of the std devs of  $u$  and  $v$ .

fields were compared to those characterized in previous studies (e.g., Pavia and O'Brien 1986; Isemer and Hasse 1991; Bauer 1996), it was found that the characterizations were in general agreement where the data used in these earlier studies were abundant, but substantial differences emerged in regions where previous studies suffered from a paucity of data. These differences were concluded to arise as a consequence of the limited sea surface wind datasets available to the earlier studies.

- Consistent with the results of earlier studies (e.g., Hennessey 1977; Justus et al. 1978; Conradsen et al. 1984; Isemer and Hasse 1991; Deaves and Lines 1997; Pang et al. 2001), it has been demonstrated that the Weibull distribution is a reasonably accurate approximation of the probability distribution of sea surface wind speeds on both a global and a local scale. The observed relationships between the estimated Weibull scale parameter  $a$  and  $\text{mean}(w)$ , and between the estimated Weibull shape parameter  $b$  and  $\text{skew}(w)$  are similar to those for a Weibull distributed variable. In particular, in those regions of the Tropics where  $\text{skew}(w)$  is negative, the ratio  $\text{mean}(w)/\text{std}(w)$  takes large values; over the Southern Ocean, where  $\text{skew}(w)$  is close to zero,  $\text{mean}(w)/\text{std}(w)$  takes values close to the 3.6 expected for an almost-Gaussian distribution, and in the NH extratropics,  $\text{mean}(w)/\text{std}(w)$  is small and  $\text{skew}(w)$  is positive.
- Despite the reasonable accuracy of the Weibull approximation, it is not an exact characterization of the PDF of sea surface wind speeds. Observed  $\text{skew}(w)$  is more strongly negative in the Tropics, and more strongly positive in the NH midlatitudes, than would be expected for a Weibull variable. A Monte Carlo simulation using synthetic Weibull datasets with numbers of degrees of freedom comparable to those of the SeaWinds data indicates that it is highly unlikely that this apparent non-Weibull behavior arises as a result of sampling fluctuations of a Weibull random variable.
- An analytic expression for the PDF of  $w$ ,  $p(w)$ , was obtained from the simple stochastic boundary layer model introduced in Monahan (2004a,b). This PDF was demonstrated to be in good qualitative agreement with the observed relationships between the mean, standard deviation, and skewness of  $w$ . In particular, the dependence of the sign of  $\text{skew}(w)$  on the ratio of  $\text{mean}(w)$  to  $\text{std}(w)$  was demonstrated to follow from the anticorrelation of the mean and skewness fields of the vector wind components discussed in Monahan (2004a,b). This anticorrelation is a consequence of the nonlinear surface drag predicted by boundary layer theory; if the surface drag is modeled as linear, the vector winds are Gaussian and the wind speed skewness is never negative. It was concluded that the Weibull distribution arises as a useful ap-

proximation to the distribution of  $w$  because it imposes the constraints on the relationship between  $\text{mean}(w)$ ,  $\text{std}(w)$ , and  $\text{skew}(w)$  that are required by the physics of the boundary layer.

- While helpful for developing a qualitative understanding of the relationships between the moments of  $w$ , the stochastic boundary layer model considered was too simple to be quantitatively useful. As well, it required as input parameters the mean and variability of a forcing function that is difficult to estimate from data. To construct more quantitatively useful expressions for the PDF of  $w$ , the PDF described in CMT, which follows from the assumption that the joint distribution of the vector wind components is bivariate Gaussian, was generalized to allow for non-zero skewness and kurtosis of the along-mean wind component  $u$  of the vector surface wind. Neglect of the skewness and kurtosis of  $u$  was shown to produce a PDF that tended to underestimate  $\text{mean}(w)$  and overestimate  $\text{std}(w)$  and was unable to reproduce the negative skewness of  $w$  observed over much of the tropical oceans. By incorporating the skewness and kurtosis of the along-mean wind component, parameterized to depend on the mean and variability of the vector wind, the errors in the representation of  $\text{mean}(w)$ ,  $\text{std}(w)$ , and  $\text{skew}(w)$  were significantly reduced. This analysis demonstrates two important points: first, that the moments of the scalar sea surface wind speed can be quite accurately predicted given a knowledge of the moments of the vector wind, and second, that the higher-order moments of the vector wind can accurately be parameterized in terms of the lower moments, as was suggested in Monahan (2004b). The grid-scale-averaged vector surface wind is a standard atmospheric general circulation model field, and parameterizations exist of the grid-scale variability of the vector wind (CMT); these quantities can be used as input to the parameterization of the PDF of  $w$  presented in this study to improve representations of grid-scale-averaged fluxes (which are in general not equal to the fluxes associated with grid-scale average winds; e.g., Mahrt and Sun 1995; Levy and Vickers 1999).

Only a single global sea surface wind dataset was considered in this study. Furthermore, the analysis was of data throughout the entire year, without consideration of seasonal variability. In Part II of this study, the quantitative details of the PDF of  $w$  are compared between seasons and with other global surface wind datasets. In general, it is found that despite quantitative differences, the qualitative features of the relationships between moments of wind speeds described in the annual

SeaWinds data are invariant between different datasets and seasons.

Given the qualitative utility of the simple stochastic boundary layer model [Eqs. (25)–(26)], an interesting extension of the present study would be the generalization of this model to include neglected processes. In particular, improved quantitative agreement between this model and observations should follow from taking into account fluctuations in the drag coefficient resulting from the effects of nonneutral stability and remote swell (Sura 2003; SS04; Monahan 2004b) and nonwhite noise structure in the forcing variability. Such an analysis would have the further benefit of contributing toward the development of physically based parameterizations of the relationships between the moments of sea surface vector wind components. Such parameterizations could then be used in empirically derived PDFs such as  $D(v, 0)$  and  $D(v, \kappa)$  instead of the statistical relationships used in this study.

Recent studies have emphasized the point that scatterometer observations do not represent the wind vector relative to a fixed coordinate system, but rather the air motion relative to the underlying sea surface. In regions of swift surface currents, the sea surface wind vector observed by the scatterometer will differ from the actual wind vector by the surface current vector (e.g., Kelly et al. 2001, 2005; Chelton et al. 2004). This fact has not been taken into account in the present study, in which the sea surface has been treated as a (rough) rigid surface. Differences between the actual sea surface wind and the SeaWinds observations may account for some of the deficiencies of the empirical and theoretical models presented in this study. An interesting direction of future study would be the contribution of surface currents to the probability distribution of sea surface winds.

A primary motivation for the study of the probability distribution of sea surface wind speeds from the perspective of climate studies is the role these distributions play in the computation of spatially and/or temporally averaged air–sea fluxes of momentum, energy, freshwater, and chemical constituents (e.g., Taylor 2000; Jones and Toba 2001; Donelan et al. 2002). The Weibull distribution provides a good empirical approximation to the PDF of  $w$  but requires knowledge of the mean and standard deviation of the wind speed. This paper has discussed both theoretical and empirical parameterizations of  $p(w)$ , which depend on vector averaged quantities of the kind naturally produced by GCMs. The incorporation of these PDFs into parameterizations of air–sea fluxes in GCMs, as discussed in CMT, presents the possibility of improving the representation of the

surface fluxes that are at the heart of the coupled physical–biogeochemical dynamics of the climate system.

*Acknowledgments.* The author acknowledges support from the Natural Sciences and Engineering Research Council of Canada, from the Canadian Foundation for Climate and Atmospheric Sciences, and from the Canadian Institute for Advanced Research Earth System Evolution Program. The author is grateful to Jim Christian and Konstantin Zahariev for helpful discussions. The author would also like to thank Philip Sura and two anonymous referees whose comments significantly improved this manuscript.

#### REFERENCES

- Abramowitz, M., and I. A. Stegun, 1972: *Handbook of Mathematical Functions*. Dover, 1046 pp.
- Atlas, R., R. Hoffman, S. Bloom, J. Jusem, and J. Ardizzone, 1996: A multiyear global surface wind velocity dataset using SSM/I wind observations. *Bull. Amer. Meteor. Soc.*, **77**, 869–882.
- Bauer, E., 1996: Characteristic frequency distributions of remotely sensed *in situ* and modelled wind speeds. *Int. J. Climatol.*, **16**, 1087–1102.
- Bentamy, A., P. Queffelec, Y. Quilfen, and K. Katsaros, 1999: Ocean surface wind fields estimated from satellite active and passive microwave instruments. *IEEE Trans. Geosci. Remote Sens.*, **37**, 2469–2486.
- Bourassa, M. A., D. M. Legler, J. J. O'Brien, and S. R. Smith, 2003: SeaWinds validation with research vessels. *J. Geophys. Res.*, **108**, 3019, doi:10.1029/2001JC001028.
- Cakmur, R., R. Miller, and O. Torres, 2004: Incorporating the effect of small-scale circulations upon dust emission in an atmospheric general circulation model. *J. Geophys. Res.*, **109**, D07201, doi:10.1029/2003JD004067.
- Chelton, D. B., and M. H. Freilich, 2005: Scatterometer-based assessment of 10-m wind analyses from the operational ECMWF and NCEP numerical weather prediction models. *Mon. Wea. Rev.*, **133**, 409–429.
- , M. G. Schlax, M. H. Freilich, and R. F. Milliff, 2004: Satellite measurements reveal persistent small-scale features in ocean winds. *Science*, **303**, 978–983.
- Conradsen, K., L. Nielsen, and L. Prahm, 1984: Review of Weibull statistics for estimation of wind speed distributions. *J. Climate Appl. Meteor.*, **23**, 1173–1183.
- Curry, J., and Coauthors, 2004: SEAFLUX. *Bull. Amer. Meteor. Soc.*, **85**, 409–424.
- Deaves, D., and I. Lines, 1997: On the fitting of low mean wind-speed data to the Weibull distribution. *J. Wind Eng. Ind. Aerodyn.*, **66**, 169–178.
- Dixon, J., and R. Swift, 1984: The dependence of wind speed and Weibull characteristics on height for offshore winds. *Wind Eng.*, **8**, 87–98.
- Donelan, M., W. Drennan, E. Saltzman, and R. Wanninkhof, Eds., 2002: *Gas Transfer at Water Surfaces*. Amer. Geophys. Union, 383 pp.
- Ebuchi, N., 1999: Statistical distribution of wind speeds and directions globally observed by NSCAT. *J. Geophys. Res.*, **104**, 11 393–11 403.
- , H. C. Graber, and M. J. Caruso, 2002: Evaluation of wind vectors observed by QuikSCAT/SeaWinds using ocean buoy data. *J. Atmos. Oceanic Technol.*, **19**, 2049–2062.
- Einstein, A., 1956: *Investigations on the Theory of Brownian Movement*. Dover, 122 pp.
- Erickson, D. J., and J. A. Taylor, 1989: Non-Weibull behavior observed in a model-generated global surface wind field frequency distribution. *J. Geophys. Res.*, **94**, 12 693–12 698.
- Fairall, C. W., E. F. Bradley, J. E. Hare, A. A. Grachev, and J. B. Edson, 2003: Bulk parameterization of air–sea fluxes: Updates and verification for the COARE algorithm. *J. Climate*, **16**, 571–591.
- Gardiner, C. W., 1997: *Handbook of Stochastic Methods for Physics, Chemistry, and the Natural Sciences*. Springer, 442 pp.
- Gradshteyn, I., and I. Ryzhik, 2000: *Table of Integrals, Series, and Products*. 6th ed. Academic Press, 1163 pp.
- Hennessey, J. P., 1977: Some aspects of wind power statistics. *J. Appl. Meteor.*, **16**, 119–128.
- Hsieh, W. W., and B. Tang, 1998: Applying neural network models to prediction and data analysis in meteorology and oceanography. *Bull. Amer. Meteor. Soc.*, **79**, 1855–1870.
- Isemer, H., and L. Hasse, 1991: The scientific Beaufort equivalent scale: Effects on wind statistics and climatological air–sea flux estimates in the North Atlantic Ocean. *J. Climate*, **4**, 819–836.
- Jet Propulsion Laboratory, cited 2001: SeaWinds on QuikSCAT Level 3: Daily, gridded ocean wind vectors. Tech. Rep. JPL PO.DAAC Product 109, California Institute of Technology. [Available online at [http://podaac.jpl.nasa.gov:2031/DATASET\\_DOCS/Qscat\\_L3.html](http://podaac.jpl.nasa.gov:2031/DATASET_DOCS/Qscat_L3.html).]
- Johnson, N., S. Kotz, and N. Balakrishnan, 1994: *Continuous Univariate Distributions*. Vol. 1. Wiley, 756 pp.
- Jondeau, E., and M. Rockinger, 2001: Gram-Charlier densities. *J. Econ. Dyn. Control*, **25**, 1457–1483.
- Jones, I. S., and Y. Toba, Eds., 2001: *Wind Stress over the Ocean*. Cambridge University Press, 307 pp.
- Justus, C., W. Hargraves, A. Mikhail, and D. Graber, 1978: Methods for estimating wind speed frequency distributions. *J. Appl. Meteor.*, **17**, 350–353.
- Kelly, K. A., 2004: Wind data: A promise in peril. *Science*, **303**, 962–963.
- , S. Dickinson, M. J. McPhaden, and G. C. Johnson, 2001: Ocean currents evident in ocean wind data. *Geophys. Res. Lett.*, **28**, 2469–2472.
- , —, and G. C. Johnson, 2005: Comparisons of scatterometer and TAO winds reveal time-varying surface currents for the tropical Pacific Ocean. *J. Atmos. Oceanic Technol.*, **22**, 735–745.
- Kestens, E., and J. L. Teugels, 2002: Challenges in modelling stochasticity in wind. *Environmetrics*, **13**, 821–830.
- Levy, G., and D. Vickers, 1999: Surface fluxes from satellite winds: Modeling air–sea flux enhancement from spatial and temporal observations. *J. Geophys. Res.*, **104**, 20 639–20 650.
- Mahrt, L., and J. Sun, 1995: The subgrid velocity scale in the bulk aerodynamic relationship for spatially averaged scalar fluxes. *Mon. Wea. Rev.*, **123**, 3032–3041.
- Meissner, T., D. Smith, and F. Wentz, 2001: A 10 year intercomparison between collocated Special Sensor Microwave Imager oceanic surface wind speed retrievals and global analyses. *J. Geophys. Res.*, **106**, 11 731–11 742.
- Monahan, A. H., 2004a: Low-frequency variability of the statistical moments of sea-surface winds. *Geophys. Res. Lett.*, **31**, L10302, doi:10.1029/2004GL019599.
- , 2004b: A simple model for the skewness of global sea surface winds. *J. Atmos. Sci.*, **61**, 2037–2049.

- , 2006: The probability distribution of sea surface wind speeds. Part II: Dataset intercomparison and seasonal variability. *J. Climate*, **19**, 521–534.
- Pang, W.-K., J. J. Forster, and M. D. Troutt, 2001: Estimation of wind speed distribution using Markov chain Monte Carlo techniques. *J. Appl. Meteor.*, **40**, 1476–1484.
- Pavia, E. G., and J. J. O'Brien, 1986: Weibull statistics of wind speed over the ocean. *J. Climate Appl. Meteor.*, **25**, 1324–1332.
- Penland, C., 2003a: Noise out of chaos and why it won't go away. *Bull. Amer. Meteor. Soc.*, **84**, 921–925.
- , 2003b: A stochastic approach to nonlinear dynamics: A review. *Bull. Amer. Meteor. Soc.*, **84**, ES43–ES52.
- Petersen, E. L., N. G. Mortensen, L. Landberg, J. Højstrup, and H. P. Frank, 1998a: Wind power meteorology. Part I: Climate and turbulence. *Wind Energy*, **1**, 25–45.
- , —, —, —, and —, 1998b: Wind power meteorology. Part II: Siting and models. *Wind Energy*, **1**, 55–72.
- Pryor, S., and R. Barthelmie, 2002: Statistical analysis of flow characteristics in the coastal zone. *J. Wind Eng. Ind. Aerodyn.*, **90**, 201–221.
- Rodwell, M., and B. Hoskins, 2001: Subtropical anticyclones and summer monsoons. *J. Climate*, **14**, 3192–3211.
- Stewart, D. A., and O. M. Essenwanger, 1978: Frequency distribution of wind speed near the surface. *J. Appl. Meteor.*, **17**, 1633–1642.
- Sura, P., 2003: Stochastic analysis of Southern and Pacific Ocean sea surface winds. *J. Atmos. Sci.*, **60**, 654–666.
- Takle, E., and J. Brown, 1978: Note on the use of Weibull statistics to characterize wind-speed data. *J. Appl. Meteor.*, **17**, 556–559.
- Taylor, P. K., Ed., 2000: Intercomparison and validation of ocean-atmosphere energy flux fields. Joint WCRP/SCOR Working Group on Air-Sea Fluxes Final Rep. WMO/TD-1036, 306 pp.
- , and M. J. Yelland, 2001: The dependence of sea surface roughness on the height and steepness of the waves. *J. Phys. Oceanogr.*, **31**, 572–590.
- Thompson, K., R. Marsden, and D. Wright, 1983: Estimation of low-frequency wind stress fluctuations over the open ocean. *J. Phys. Oceanogr.*, **13**, 1003–1011.
- Tuller, S. E., and A. C. Brett, 1984: The characteristics of wind velocity that favor the fitting of a Weibull distribution in wind speed analysis. *J. Climate Appl. Meteor.*, **23**, 124–134.
- Wanninkhof, R., 1992: Relationship between wind speed and gas exchange over the ocean. *J. Geophys. Res.*, **97**, 7373–7382.
- , and W. R. McGillis, 1999: A cubic relationship between air-sea CO<sub>2</sub> exchange and wind speed. *Geophys. Res. Lett.*, **26**, 1889–1892.
- , S. C. Doney, T. Takahashi, and W. R. McGillis, 2002: The effect of using time-averaged winds on regional air-sea CO<sub>2</sub> fluxes. *Gas Transfer at Water Surfaces*, M. A. Donelan et al., Eds., Amer. Geophys. Union, 351–356.
- Wentz, F., S. Peteherych, and L. Thomas, 1984: A model function for ocean radar cross sections at 14.6 GHz. *J. Geophys. Res.*, **89**, 3689–3704.
- Wright, D. G., and K. R. Thompson, 1983: Time-averaged forms of the nonlinear stress law. *J. Phys. Oceanogr.*, **13**, 341–345.
- Yuan, X., 2004: High-wind-speed evaluation in the Southern Ocean. *J. Geophys. Res.*, **109**, D13101, doi:10.1029/2003JD004179.